Polymer Chemistry

ROYAL SOCIETY OF CHEMISTRY

PAPER

View Article Online
View Journal | View Issue

Check for updates

Cite this: *Polym. Chem.*, 2024, **15**, 999

Metal-catalyzed stereoselective ring-opening polymerization of functional β-lactones: methylene-alkoxy-fluorinated polyhydroxyalkanoates unveil the role of non-covalent interactions†

Ali Dhaini,[a] Rama M. Shakaroun,[a] Ali Alaaeddine,[b] Jean-François Carpentier *[a] and Sophie M. Guillaume *[a]

Non-covalent interactions (NCIs) can play a major role in the stereoselective ring-opening polymerization (ROP) of racemic β-lactones mediated by achiral metal catalysts, towards the formation of the corresponding polyhydroxyalkanoates (PHAs) with a specific microstructure. Our longstanding endeavor to better understand the factors governing the stereoselective ROP of 4-substituted β-propiolactone monomers *rac*-BPL^{FG}s (resulting in PBPL^{FG}s; FG = (non)functional group), from catalyst systems based on diamino- or amino-alkoxy-bis(*ortho*,*para*-substituted)phenolate rare earth complexes associated with an exogenous alcohol as an initiator, indicated that the formation of iso-enriched polyesters requires the use of *ortho*-halogen-substituted phenolate ligands (halogen = F, Cl, and Br) along with a methylene alkoxide pending substituent (FG = $-CH_2OCH_2R^*$) on the lactone. Any other ligand/β-lactone combination resulted in either syndiotactic or atactic PBPL^{FG}s. We report herein the controlled ROP of 4-methylene-alkoxy-fluorinated substituted β-propiolactone, *rac*-BPL^{CH_2OCF_2CHF_2}, catalyzed by diamino-bis(*ortho*,*para*-R,R-substituted)phenolate yttrium catalyst systems Y{ONNO^{R2}}/*i*PrOH (with R = Me, Cl, *t*Bu, cumyl; namely **1a–d**/*i*PrOH, respectively). This monomer does not feature any outer methylene hydrogen in the alkoxide moiety ($-CH_2O\underline{C}\underline{F}_2CHF_2$ *vs.* $-CH_2O\underline{C}\underline{H}_2R^*$), thus enabling the evaluation of the role of outer $CH_2O(R^*)\underline{C}\underline{H}_2\cdots R$ NCIs in the stereocontrol. The *t*Bu catalyst **1c** showed the highest ROP activity (TOF up to 4650 h^{-1}) out of the four catalyst systems investigated. The fluoroalkyl PHAs were recovered with molar mass values up to $M_{n,NMR}$ = 106 000 g mol^{-1} and narrow dispersity ($Đ_M$ = 1.02–1.24). Detailed NMR and mass spectrometry characterization studies supported the formation of α-isopropoxy,ω-hydroxy telechelic PBPL^{CH_2OCF_2CHF_2} chains. Catalysts **1c** and **1d** flanked with bulky phenolate substituents (R = *t*Bu, cumyl) and the chloro-substituted one **1b** all returned syndio-enriched PBPL^{CH_2OCF_2CHF_2}s with P_r up to 0.87, as assessed by ^{13}C NMR spectroscopy. Only the methyl substituted catalyst **1a** gave atactic PHAs. Eventually, these findings support the hypothesis that both inner and outer methylene hydrogens within an alkoxymethylene exocyclic group on the *rac*-β-lactone monomer ($\underline{C}\underline{H}_2O\underline{C}\underline{H}_2R^*$) are required, along with an *ortho*-chloro-substituted yttrium bisphenolate catalyst (Y{ONNO^{Cl_2}}), to induce NCIs ($Cl\cdots\underline{H}_2\underline{C}$-O-$\underline{C}(R^*)\underline{H}_2\cdots Cl$), ultimately resulting in unique isotactic synthetic PHAs.

Received 30th December 2023,
Accepted 27th January 2024

DOI: 10.1039/d3py01430d

rsc.li/polymers

Introduction

The ring-opening polymerization (ROP) of chiral cyclic esters into the corresponding polyesters that exhibit stereoregularity along their backbone is highly desirable. Such polymers exhibiting adjacent stereocenters having the same (isotactic structure), or opposite/alternating (syndiotactic/heterotactic structure) configuration, are indeed valuable for their tunable thermal, mechanical and degradation properties, in comparison with those exhibiting randomly distributed stereocenters

[a]*Univ. Rennes, CNRS, Institut des Sciences Chimiques de Rennes, UMR 6226, F-35042 Rennes, France. E-mail: jean-francois.carpentier@univ-rennes.fr, sophie.guillaume@univ-rennes.fr*
[b]*Univ. Libanaise, Campus Universitaire Rafic Hariri Hadath, Faculté des Sciences, Laboratoire de Chimie Médicinale et des Produits Naturels, Beirut, Lebanon*
† Electronic supplementary information (ESI) available. See DOI: https://doi.org/10.1039/d3py01430d

(atactic structure).[1–4] Such polyesters typically include polylactide (PLA) and polyhydroxyalkanoates (PHAs), which are commonly prepared by ROP of lactide (LA) and β-lactones, respectively. One advantage (among others), over PLA, of the most common synthetic PHAs, which are derived from 4-substituted β-propiolactones (namely BPL^{FG}s, FG = non-functional or functional group), arises from the FG exocyclic side chain. Indeed, the desired functionality can be easily introduced into monomers by chemical modification, ultimately resulting in a large range of functional PBPL^{FG}s with correspondingly diverse and tunable properties. Ideally, such stereoregular (isotactic, syndiotactic or heterotactic) PLAs and PHAs are more attractive if they can be obtained from a racemic mixture of enantiopure monomers, namely from racemic lactide and β-propiolactones (*rac*-LA and *rac*-BPL^{FG}s), respectively, provided a stereoselective catalyst system is used.[5–8]

Through our ongoing interest in promoting the formation of well-defined PLA and PHAs with controlled stereoregularity, we have established that achiral tetradentate diamino- or amino-alkoxy-bis(*ortho*,*para*-R,R-substituted)phenolate rare earth metal (M) complexes associated with an exogenous alcohol as a co-initiator (typically isopropanol), namely M{ONXO^{R2}}/*i*PrOH (with X = OMe or NMe$_2$), effectively promote the stereoselective ROP of *rac*-LA and *rac*-BPL^{FG}s.[9]

Moderately-to-highly heterotactic PLA (P_r = 0.56–0.96; $P_{r/m}$ = probability of *racemo*/*meso* enchainment between adjacent monomer units as determined by ^{13}C NMR, with $P_r + P_m = 1$; P_r is identical to P_{syndio} and P_m is identical to P_{iso}; $P_m = 1$ or $P_r = 1$ for a perfectly isotactic or syndiotactic polymer, respectively, and $P_r = P_m = 0.5$ for an atactic one) was prepared from the ROP of *rac*-LA promoted at room temperature using a rare earth amido complex (M = La, Nd, Y) featuring amino-alkoxy-bisphenolate ligands with various *ortho*-R and *para*-R substituents {ONOO^{R2}}$^{2-}$. The bulkier the substituents on the metal ancillary ligand (R = Me ≪ *t*Bu < adamantyl < CMe$_2$Ph < CMe$_2$*t*Bu < CPh$_3$), the more hetero-enriched the PLAs. This initial study also revealed that the smaller yttrium (ionic radius: Y < Nd < La) afforded significantly higher stereoselectivity over the larger neodymium or lanthanum (P_r = 0.91, 0.65, and 0.60, respectively). Also, the stereoelectronic contribution of the remote phenolate *para*-R substituents was demonstrated to not significantly impact the control of LA unit enchainment.[9] Accordingly, we later focused our efforts on the more easily synthetically accessible bisphenolate complexes flanked with identical *ortho*,*para*-R,R substituents, using preferentially yttrium complexes, namely Y{ONXO^{R2}}/*i*PrOH catalyst systems.

The extended series of 4-substituted β-propiolactones that we have been investigating using these latter catalyst systems aimed at covering a wide range of exocyclic substituents, in order to probe the contribution of stereoelectronically diverse lactone side-chains to the stereocontrol of the ROP. Thus, alkyl (FG = Me), (di)methylene (thio)alkoxide (FG = CH$_2$OMe, CH$_2$O*i*Pr, CH$_2$O*t*Bu, CH$_2$OAll, CH$_2$OBn, CH$_2$OSi*t*BuMe$_2$, CH$_2$OPh, CH$_2$SPh, and CH$_2$CH$_2$OBn), and ester (FG = CO$_2$Me, CO$_2$All, and CO$_2$Bn) substituted β-propiolactones enabled the estimation of the influence of short/long, polar/non-polar, alkyl/functional lactone pending groups on their ROP mediated by the Y{ONXO^{R2}}/*i*PrOH catalyst platform (Scheme 1).[7–9,10–17] Extended insights into the stereoselectivity of the resulting PHAs by ^{13}C NMR analyses first suggested that, by itself, neither the length, steric bulkiness, electronic environment nor chemical functionality (alkyl *vs.* ether *vs.* ester) provided by the FG exocyclic substituent, may enable the preparation of PHAs other than atactic or syndiotactic PHAs. While the chemical synthesis of syndiotactic PHAs – that arise from a regular "chain-end stereocontrol mechanism" thanks to the sterically bulky substituents installed on the ligand of the catalyst,[5,7–17] and that otherwise cannot be found as natural polymers since the PHAs produced naturally or biosynthetically from microorganisms or enzymes are invariably isotactic polymers – was thereby rewardingly established, isotactic polymers were only exceptionally obtained from these Y{ONXO^{R2}}/*i*PrOH catalyst systems.[18] Indeed, only the 4-alkoxymethylene-substituted β-propiolactones, simultaneously featuring inner and outer methylene groups apart from the side-chain oxygen atom, namely *rac*-BPL$^{\underline{CH_2}O\underline{CH_2}R^*}$ (R* = H, CH=CH$_2$, Ph), returned the isotactic corresponding PBPL$^{\underline{CH_2}O\underline{CH_2}R^*}$s, provided the yttrium bisphenolate ligand was bearing *ortho*-halogen substituents (R = F, Cl, Br).[11,15] DFT insights corroborated these experimental observations upon evidencing the formation of "second-sphere" interactions, referred to as non-covalent interactions (NCIs), between the phenolate *ortho*-halogen and the acidic hydrogens from both the inner and outer methylenes on the last inserted monomer unit (*Cl*···$\underline{H_2}$C-O-$\underline{C}$(R*)$\underline{H_2}$···*Cl*), *i.e.*, on the repeating unit closest to the metal center and its surrounding ligand. Of note, these computational results emphasized the negligible role of the phenolate *para*-substituents that are unlikely to be involved in NCIs with the monomer exocyclic side chain, as they are sterically too distant from this active site. Furthermore, this *in silico* information suggested that, besides, yet in complement of, the stereoelectronic environment in close proximity of the active center, such as (ligand)*Cl*···$\underline{H_2}$C-O NCIs that are attractive in nature, is essential to drive the catalyst isoselectivity.[18*d*,19–24]

Interestingly, stereoregular PHAs have also been prepared by ROP of the eight-membered R-substituted cyclic diolide (DL^R).[25] Rewardingly, ROP of *rac*-DL^{Me} mediated by yttrium-salen complexes generated perfectly isotactic well-defined high molar mass PDL^{Me} (aka PHB, poly(3-hydroxybutyrate), with P_m > 0.99, M_n = 154 000 g mol^{-1} and $Đ_M$ = 1.01).[26] Isotactic PHA copolymers were similarly produced from the ring-opening copolymerization of *rac*-DL^{Me} with *rac*-DL$^{R'}$ (R′ = Et, *n*Bu) (P_m > 0.99) or through the design of unsymmetrically disubstituted eight-membered diolides *rac*-DL$^{R,R'}$, with R ≠ R′, returning alternating isotactic PHAs.[27–29] Syndiotactic stereodiblock PHAs were also successfully obtained from the ROP of *meso*-DL^R diastereomers (Scheme 2).[30]

Of note, amino-alkoxy-bisphenolate yttrium catalyst systems have also been successfully reported to give stereoregular polymers from the ROP of other racemic cyclic monomers. These

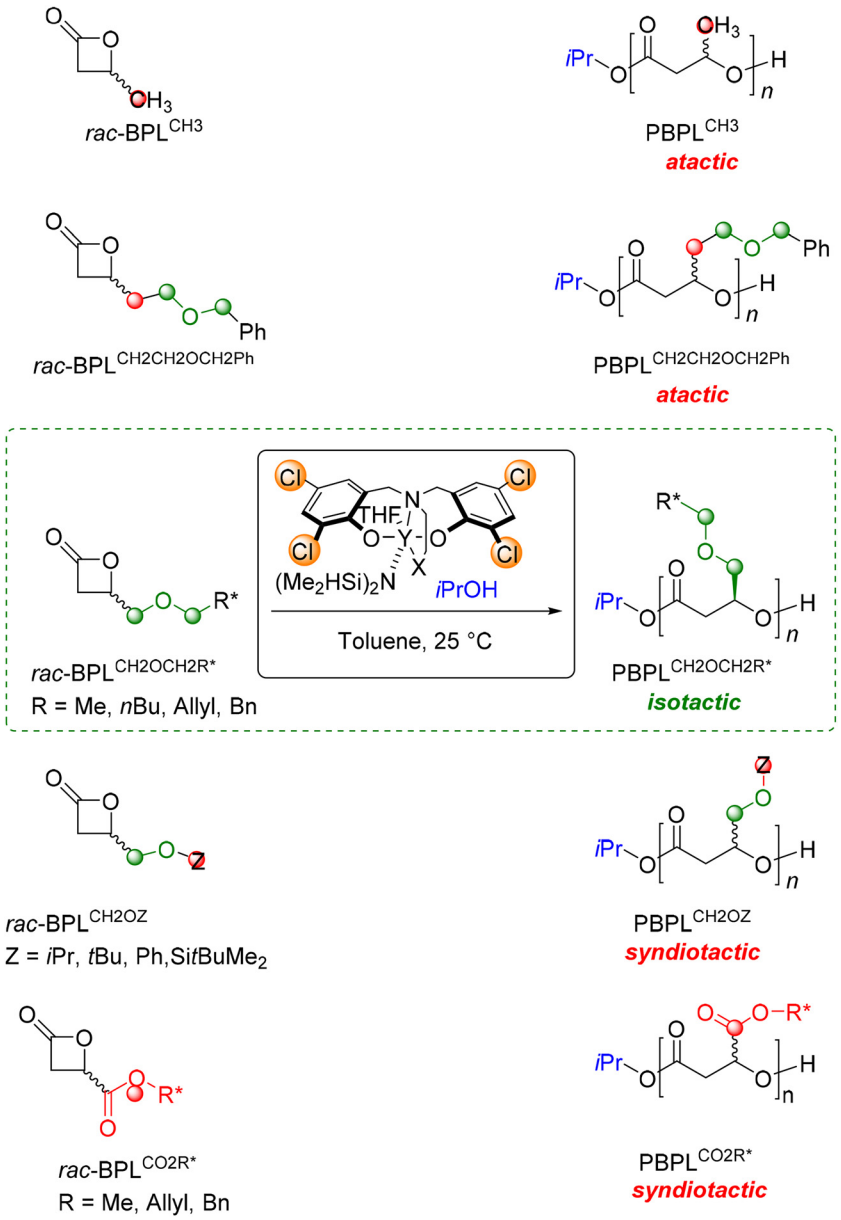

Scheme 1 Stereoselective ROP of various chiral *racemic* 4-substituted-β-propiolactones, *rac*-BPL^{FG}s (FG = Me, $CH_2CH_2OCH_2Ph$, $CH_2OCH_2R^*$ with R* = Me, *n*Bu, allyl, Bn, CH_2OZ with Z = *i*Pr, *t*Bu, Ph, Si*t*BuMe$_2$, CO_2R^* with R* = Me, Allyl, Bn) performed with Y{ONXO^{Cl_2}}/*i*PrOH catalyst systems, illustrating the importance of the $-CH_2OCH_2R^*$ exocyclic side chain to impart stereoregularity on these dichloro-substituted bisphenolate yttrium catalysts.[9,11–17]

include the five-membered γ-butyrolactone (GBL), the six-membered ring δ-valerolactone, and the related fused six-five bicyclic lactones, namely 3,4-*trans*-cyclohexyl and 4,5-*trans*-cyclohexyl fused γ-butyrolactones, respectively. Similarly, ROP of glycolide (GA), lactide/glycolide, and *O*-carboxyanhydride (OCA) monomers with such yttrium-based catalyst systems has been reported to provide stereoregular poly(α-hydroxyalkanoate)s[5–7,31] and references therein.

In order to further verify our above-mentioned hypothesis of an intimate stereoelectronic relationship between the β-lactone exocyclic substituent and the suitable yttrium R ancillary substituents, which can impart isoselectivity in the ROP of 4-substituted *rac*-BPL$^{CH_2OCH_2R^*}$, we thus report herein the ROP of the 4-methylene-alkoxy-fluorinated substituted β-propiolactone, *rac*-BPL^{CH_2OCF_2CHF_2}. The ROP reactions were conducted using diamino-bisphenolate yttrium catalyst systems Y{ONNO^{R2}}/*i*PrOH bearing various *ortho,para*-R,R substituents (R = Me, Cl, *t*Bu, CMe_2Ph, namely **1a–d**/*i*PrOH) (Scheme 3). In *rac*-BPL^{CH_2OCF_2CHF_2}, the outer methylene hydrogens are replaced by fluorine in order to inhibit the outer O$\underline{C}$R*$\underline{H_2}\cdots Cl$(ligand) NCIs, and ultimately to evaluate the impact of such an interaction on the resulting PHA stereo-

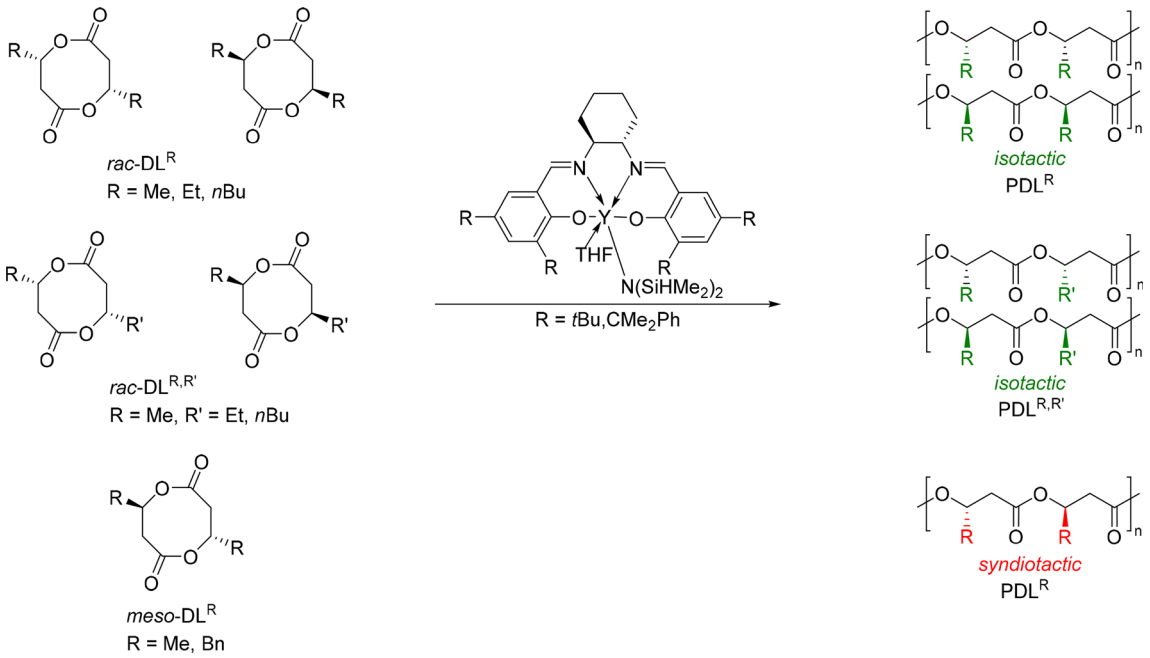

Scheme 2 Yttrium-salen-mediated stereoselective ROP of *rac*- and *meso*-DL$^{R/R'}$s (R/R′ = Me, Et, *n*Bu, Bn) producing stereoregular isotactic or syndiotactic PHAs.[25–30]

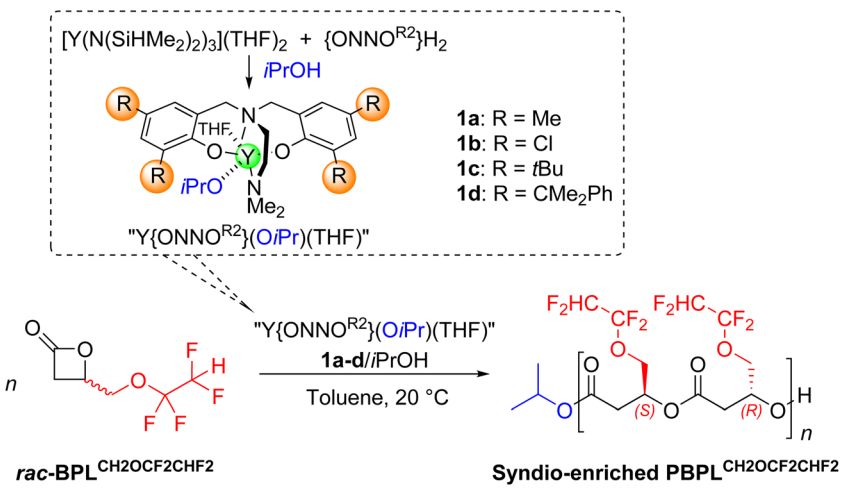

Scheme 3 Stereoselective ROP of *racemic* 4-((2,2,3,3-tetrafluoropropyl)methylene) β-propiolactone, *rac*-BPL^{CH_2OCF_2CHF_2}, catalyzed by diaminobisphenolate yttrium complexes Y{ONNO^{R2}} **1a–d** in the presence of *i*PrOH as the co-initiator.

regularity. Hence, the ROP of *rac*-BPL^{CH_2OCF_2CHF_2} was studied: (i) to determine and rationalize the activity of catalysts, especially in relation to the stereoelectronic effects of the phenolate R substituents, (ii) to fully characterize the resulting PBPL^{CH_2OCF_2CHF_2}s at the molecular and microstructural levels by NMR spectroscopy, SEC, mass spectrometry, DSC and TGA thermal analyses, and (iii) finally to assess the catalyst ability in affording stereoregular PHAs. Ultimately, the suggested contribution of the combined stereoelectronic parameters and involvement of NCIs to the control of stereoregularity of the resulting PHAs was successfully verified.

Fluorinated polymers are attractive for their thermal, chemical and electronic stabilities. They are typically very hydrophobic, not flammable, inert to acids, bases, solvents, and oils, and highly resistant to aging and oxidation, and exhibit low dielectric constants, low refractive indexes and low surface tension. Ranging from semi-crystalline to amorphous forms and from thermoplastic to elastomeric materials, they have found various applications from building and construction, automotive, petrochemical, aeronautics and aerospace, photonics, electronics, and biomedical systems. Side-chain fluorinated polymers are valuable for their surface properties

and are often employed as polymer dispersions in water used as coatings applied to textiles, carpets, nonwovens and paper to provide water, soil, oil and stain resistance.[32–35] In addition, to our knowledge, besides microbial PHAs containing fluorinated side-chain substituents,[36–38] there are only two examples of chemically synthesized PHAs featuring a fluorinated pendant substituent on the repeating units or a fluorinated end-capping group, which are still being obtained by post-polymerization functionalization.[39,40] While the novel PBPL^{CH_2OCF_2CHF_2}s reported herein add to the previously established short series of fluoroalkyl PHAs, all of which were atactic polymers,[41] they represent the first extended series of stereoregular fluorinated PHAs chemically prepared by ROP of a β-lactone monomer.

Experimental section

Methods and materials

All manipulations involving organometallic catalysts were performed under an inert atmosphere (argon, <3 ppm O_2) using standard Schlenk, vacuum line, and glovebox techniques. Solvents were freshly distilled from Na/benzophenone under argon and degassed thoroughly by freeze–thaw–vacuum cycles prior to use. Isopropyl alcohol (Acros) was distilled over Mg turnings under an argon atmosphere and placed over activated 3–4 Å molecular sieves. Bisphenol proligands {ONXO^{R2}}H_2, yttrium amide precursors Y[N(SiHMe$_2$)$_2$]$_3$(THF)$_2$ of **1a–d**,[10,42] [Salph(Cr(THF)$_2$)][Co(CO)$_4$][43–45] and (BDI)ZnN(SiMe$_3$)$_2$ [46,47] (BDI = β-diketiminate) were synthesized according to the literature procedure. *Racemic* 2-((1,1,2,2-tetrafluoroethoxy)methyl) oxirane (*rac*-G^{CH_2OCF_2CHF_2}) (ABCR) was dried over CaH_2 and then stored under argon at −27 °C (^{1}H, J-MOD and ^{19}F NMR data – refer to Fig. S2–S4†). Enantioenriched (*S*)-G^{CH_2OCF_2CHF_2} (>90% ee) was prepared as a colorless oil (1.6 g, 40%) by hydrolytic kinetic resolution (HKR) of *rac*-G^{CH_2OCF_2CHF_2}, following a reported procedure (refer to the ESI, Scheme S1 and Fig. S1†).[48] All other reagents were purchased from Aldrich, Sigma or Acros and used as received.

Instrumentation and measurements

^{1}H (500 and 400 MHz), ^{13}C{^{1}H} (125 and 100 MHz) and 2D (COSY, HMBC, HSQC, and DOSY) NMR spectra were recorded on Bruker Avance AM 500 or Ascend 400 spectrometers at 25 °C. ^{1}H and ^{13}C{^{1}H} NMR spectra were referenced internally relative to $SiMe_4$ (δ 0 ppm) using the residual solvent resonances. Coupling constants are reported in Hz.

Monomer conversions were calculated from the ^{1}H NMR spectra of the crude polymer samples in $CDCl_3$ or $(CD_3)_2CO$ by using the integration (Int.) ratios Int.$_{PBPL(CH_2OCF_2CHF_2)}$/[Int.$_{PBPL(CH_2OCF_2CHF_2)}$ + Int.$_{BPL(CH_2OCF_2CHF_2)}$] of the methine hydrogen signal of BPL^{CH_2OCF_2CHF_2} and PBPL^{CH_2OCF_2CHF_2} (the corresponding methine hydrogen signal of the polymer (see above) and of the monomer δ (ppm) 4.71).

Chiral gas chromatography analysis of (*S*)-G^{CH_2OCF_2CHF_2} was performed on a GC/FID VARIAN CP-3380 chromatograph equipped with a Chiralsil-Dex CB Varian CP7502 Chrompack.

Number-average molar mass ($M_{n,SEC}$), weight-average molar mass ($M_{w,SEC}$) and dispersity ($Đ_M = M_w/M_n$) values of the PBPL^{FG}s were determined by size-exclusion chromatography (SEC) in THF at 30 °C (flow rate = 1.0 mL min^{-1}) on Polymer Laboratories PL50 apparatus equipped with a refractive index detector and a set of two ResiPore PLgel 3 μm MIXED-D 300 × 7.5 mm columns. The polymer samples were dissolved in THF (5 mg mL^{-1}). All elution curves were calibrated with polystyrene standards (M_p = 290 300, 126 000, 70 500, 30 230, 19 920, 9960, 4900, 3320, 1180, and 580 g mol^{-1}); $M_{n,SEC}$ values of the PBPL^{FG}s were uncorrected for the possible difference in the hydrodynamic radius *vs.* those of polystyrene.

The molar mass of PBPL^{FG} samples was also determined by ^{1}H NMR analysis in $CDCl_3$ or $(CD_3)_2CO$ from the relative intensities of the signals of the PBPL^{CH_2OCF_2CHF_2} repeating unit methine hydrogen (δ (ppm): 5.48 –OC*H*($CH_2OCF_2CHF_2$)CH_2), and the isopropyl chain-end (δ (ppm): 4.98 $(CH_3)_2CHO$–, 1.21 $(CH_3)_2$CHO–).

High resolution matrix-assisted laser desorption ionization-time of flight, MALDI-ToF, mass spectra of the polymers were recorded using an ULTRAFLEX III TOF/TOF spectrometer (Bruker Daltonik Gmbh, Bremen, Germany) in positive ionization mode. Spectra were recorded using reflectron mode and an accelerating voltage of 25 kV. A mixture of a freshly prepared solution of the polymer in THF or CH_2Cl_2 (HPLC grade, 10 mg mL^{-1}) and DCTB (*trans*-2-(3-(4-*tert*-butylphenyl)-2-methyl-2-propenylidene)malononitrile), and a MeOH solution of the cationizing agent (NaI, 10 mg mL^{-1}) was prepared. These solutions were combined in a 1 : 1 : 1 v/v/v ratio of matrix-to-sample-to-cationizing agent. The resulting solution (*ca.* 0.25–0.5 μL) was deposited onto the sample target (Prespotted AnchorChip PAC II 384/96 HCCA) and air or vacuum dried.

Differential scanning calorimetry (DSC) analyses were performed with a DSC2500 TA Instrument calibrated with indium, at a rate of 10 °C min^{-1}, under a continuous flow of helium (25 mL min^{-1}), using aluminum capsules (40 μL). The thermograms were recorded according to the following cycles: −80 to +200 °C at 10 °C min^{-1}; +200 to −80 °C at 10 °C min^{-1}; −80 °C for 5 min; −80 to +200 °C at 10 °C min^{-1}; +200 to −80 °C at 10 °C min^{-1}. Melting-transition (T_m) and glass-transition (T_g) temperatures were measured from the second heating run.

Thermogravimetric analyses (TGA) were performed on a Mettler Toledo TGA/DSC1 by heating the polymer samples at a rate of 10 °C min^{-1} from +25 to +500 °C under a dynamic nitrogen atmosphere (flow rate = 10 mL min^{-1}). The onset decomposition temperature (T_d) was defined as the temperature for 5% weight loss.

Carbonylation of *racemic* 2-((1,1,2,2-tetrafluoroethoxy) methyl)oxirane (*rac*-G^{CH_2OCF_2CHF_2}) into *racemic* 4-((1,1,2,2-tetrafluoroethoxy)methyl)oxetan-2-one (*rac*-BPL^{CH_2OCF_2CHF_2}).[41,49] The procedure used was adapted from a previously reported

synthesis, especially for the purification of epoxide (previously performed by distillation at 70 °C) and scale-up synthesis (0.96 g, 79%).[41] In a typical experiment, in a glovebox, a Schlenk flask was charged with [Salph(Cr(THF)$_2$)][Co(CO)$_4$] (248 mg, 0.274 mmol). On a vacuum line, dry DME (15 mL) was syringed in and the resulting solution was cannulated into a degassed high-pressure stainless steel reactor, which was pressurized with carbon monoxide (30 bars), and stirred with a magnetic bar for 15 min before depressurization. A solution of *rac*-G^{CH_2OCF_2CHF_2} (3.01 g, 17.28 mmol, 63 equiv. *vs.* Cr) in dry DME (15 mL) was transferred into the reactor, which was then pressurized with CO to 40 bars. The reaction mixture was stirred for 2 days at 20 °C. The reactor was then vented to atmospheric pressure, volatiles were removed under vacuum and the crude product was purified through a silica column (CH_2Cl_2, 2 × 300 mL). Evaporation of volatiles afforded 4-((1,1,2,2-tetrafluoroethoxy)methyl)oxetan-2-one, *rac*-BPL^{CH_2OCF_2CHF_2}, as a yellowish oil (2.60 g; 75%). ^{1}H NMR (400 MHz, $(CD_3)_2CO$, 25 °C) δ (ppm): 6.27 (tt, $^3J_{H-F}$ = 3.0, $^2J_{H-F}$ = 52.0, 1H, OCF$_2$C*H*F$_2$), 4.87 (m, 2H, *CH*$_2$OCHF$_2$), 4.47 (dd, $^3J_{H-H}$ = 4.4, $^2J_{H-H}$ = 12.0, 1H, CHC*H*H*O*), 4.36 (dd, $^3J_{H-H}$ = 5.5, $^2J_{H-H}$ = 12.0, 1H, CHC*H*HO), 3.65 (dd, $^3J_{H-H}$ = 6.0, $^2J_{H-H}$ = 17.0, 1H, C(O)CH*H*CH), 3.43 (dd, $^3J_{H-H}$ = 4.0, $^2J_{H-H}$ = 16.5, 1H, C(O)C*H*HCH) (Fig. S5†). ^{13}C J-MOD NMR (125 MHz, $(CD_3)_2CO$, 25 °C) δ (ppm): 167.7 (*C*=O), 118.4 (O*C*F$_2$CF$_2$H), 109.0 (tt, $^1J_{C-F}$ = 247, $^2J_{C-F}$ = 40, OCF$_2$*C*F$_2$H), 68.5 (*C*HOC(O)), 65.3 ($^4J_{H-F}$ = 5, *C*H$_2$OCF$_2$), 40.4 (OC(O)*C*H$_2$CH) (Fig. S6†). ^{19}F NMR (376 MHz, $(CD_3)_2CO$, 25 °C) δ (ppm): −138.4 (dt, $^2J_{H-H}$ = 52.7, $^3J_{F-F}$ = 5.6, 2F, OCF$_2$C*F*$_2$H), −92.3 (dt, $^3J_{F-H}$ = 3.0, $^3J_{F-F}$ = 5.6, 2F, OC*F*$_2$CF$_2$H) (Fig. S7†).

The carbonylation of (*S*)-2-((1,1,2,2-tetrafluoroethoxy) methyl)oxirane (>90% ee) was performed similarly and (*S*)-BPL^{CH_2OCF_2CHF_2} (>90% ee) was obtained as a colorless oil (0.59 g, 74%), which NMR spectra were identical to those of *rac*-BPL^{CH_2OCF_2CHF_2} (Fig. S2–S4†). Both *rac*-BPL^{CH_2OCF_2CHF_2} and (*S*)-BPL^{CH_2OCF_2CHF_2} were stored under argon in a fridge at −4 °C.

Typical *rac*-BPL^{CH_2OCF_2CHF_2} polymerization procedure[10–17]

In a typical experiment (Table 1, entry 4), in a glovebox, a Schlenk flask was charged with [Y(N(SiHMe$_2$)$_2$)$_3$](THF)$_2$ (8.8 mg, 14.0 μmol) and {ONNO^{tBu2}}H$_2$ (**1c**, 6.2 mg, 9.8 μmol), and toluene (0.4 mL) was next added. To this solution, *i*PrOH (75.7 μL of a 1% (v/v) solution in toluene, 1 equiv. *vs.* Y) was added under stirring at room temperature (*ca.* 20 °C). After 5 min of stirring, a solution of *rac*-BPL^{CH_2OCF_2CHF_2} (200 mg, 0.98 mmol, 100 equiv. *vs.* Y) in toluene (0.5 mL) was added rapidly and the mixture was stirred at 20 °C overnight (Fig. 1

Table 1 Characteristics of the PBPL^{CH_2OCF_2CHF_2}s synthesized by ROP of *rac*-BPL^{CH_2OCF_2CHF_2} mediated by **1a–d**/*i*PrOH catalyst systems[a]

Entry	Catalyst	Solvent	$[M]_0/[\mathbf{1}]_0$ [a]	Time[b] (h)	Conv.[c] (%)	TOF[d] (h^{-1})	$M_{n,theo}$ [e] (g mol^{-1})	$M_{n,NMR}$ [f] (g mol^{-1})	$M_{n,SEC}$ [g] (g mol^{-1})	$Đ_M$ [g]	P_r [h]	T_g [i] (°C)
1	**Zn** [j]	Toluene	100	15.75	82	5.2	16 500	14 800	9100	1.03	0.45	−25.0
2	**1d** [k]	Toluene	100	27	100	>3.7	20 200	14 200	13 000	1.07	0.09	−7.8[k]
3	**1a**	Toluene	50	48	100	>1.0	10 100	7500	9300	1.12	0.57	−20.7
4	**1a**	Toluene	100	46	47	1.0	9500	6200	5300	1.43	0.53	n.o.[l]
5	**1b**	Toluene	50	16	100	>6.2	10 100	8100	8400	1.06	0.77	−19.2
6	**1b**	Toluene	100	29	97	>3.3	20 000	15 500	16 200	1.15	0.69	−17.4
7	**1b**	Toluene	100	18	100	>5.5	20 200	21 800	17 400	1.14	0.74	−11.9
8	**1c**	Toluene	60	0.5	97	116	11 800	11 200	11 200	1.04	0.86	−22.8
9	**1c**	Toluene	60	3 min	94	1128	11 500	10 900	11 600	1.06	0.85	−19.4
10	**1c**	Toluene	100	18.5	100	>5.4	20 200	16 000	11 800	1.03	0.79	−22.9
11	**1c**	Toluene	250	30 s	13	3900	6700	7100	9500	1.05	0.73	−16.8
12	**1c**	Toluene	250	1 min	31	4650	15 700	13 800	14 200	1.02	0.85	−15.6
13	**1c**	Toluene	250	2 min	49	3675	24 700	24 500	25 300	1.04	0.83	−13.6
14	**1c**	Toluene	250	5 min	54	1620	27 400	20 900	25 300	1.05	0.84	−14.4
15	**1c**	Toluene	250	6	100	>41.6	50 600	53 600	61 600	1.09	0.79	−7.5
16	**1c**	Toluene	500	4	100	>125	101 100	106 000	102 600	1.24	0.79	−5.8
17	**1d**	Toluene	50	2	100	>25	10 100	10 900	11 400	1.05	0.85	−17.0
18	**1d**	Toluene	100	27.3	100	>3.7	20 200	16 500	12 900	1.07	0.86	−17.9
19	**1b**	C_6H_5Cl	50	72	100	>0.7	10 100	6500	13 000	1.06	0.67	n.d.[m]
20	**1d**	C_6H_5Cl	100	1	100	>100	20 200	21 500	14 500	1.13	0.87	n.d.[m]
21	**1b**	THF	20	48	24	0.1	1300	1100	800	1.02	0.59	n.d.[m]
22	**1b**	THF	100	29	17	0.6	3560	2200	2500	1.21	0.66	n.d.[m]
23	**1d**	THF	100	29	48	1.6	9700	5300	5000	1.09	0.83	n.d.[m]

[a] Reactions performed with $[BPL^{CH_2OCF_2CHF_2}]_0 = [M]_0$ = 1.0 M in toluene, with $[\mathbf{1}]_0/[i\text{PrOH}]_0$ = 1, at room temperature. [b] Reaction times were not necessarily optimized. [c] Conversion of BPL^{CH_2OCF_2CHF_2} as determined by ^{1}H NMR analysis of the crude reaction mixture. [d] Unoptimized turnover frequency, in mol(BPL^{CH_2OCF_2CHF_2}) mol(Y)$^{-1}$ h^{-1}, as determined from TOF = conversion × $[M]_0/[\mathbf{1}]_0$/reaction time. [e] Molar mass calculated according to $M_{n,theo} = ([BPL^{CH_2OCF_2CHF_2}]_0/[\mathbf{1}]_0 \times \text{conv.}_{BPLCH_2OCF_2CHF_2} \times M_{BPLCH_2OCF_2CHF_2}) + M_{i\text{PrOH}}$ with $M_{BPLCH_2OCF_2CHF_2}$ = 202 g mol^{-1} and $M_{i\text{PrOH}}$ = 60 g mol^{-1}. [f] Molar mass determined by ^{1}H NMR analysis of the isolated polymer, from the resonances of the terminal O*i*Pr group. [g] Number-average molar mass (uncorrected values) and dispersity ($Đ_M = M_w/M_n$) determined by SEC analysis in THF at 30 °C *vs.* polystyrene standards. [h] P_r is the probability of *racemic* linkages between BPL^{CH_2OCF_2CHF_2} units as determined by ^{13}C{^{1}H} NMR analysis of the isolated PBPL^{CH_2OCF_2CHF_2} (refer to the Experimental section). [i] Glass transition temperature as determined by DSC analysis. [j] Zn = (BDI)Zn(N(SiMe$_3$)$_2$)/*i*PrOH. [k] ROP of enantioenriched (*S*)-BPL^{CH_2OCF_2CHF_2} (>90% ee) that gives an isotactic-rich polymer[50] with T_m = 101.9 °C, T_c = 67.2 °C and ΔH_m = 0.42 J g^{-1}. [l] n.o.: no signal observed. [m] n.d.: not determined.

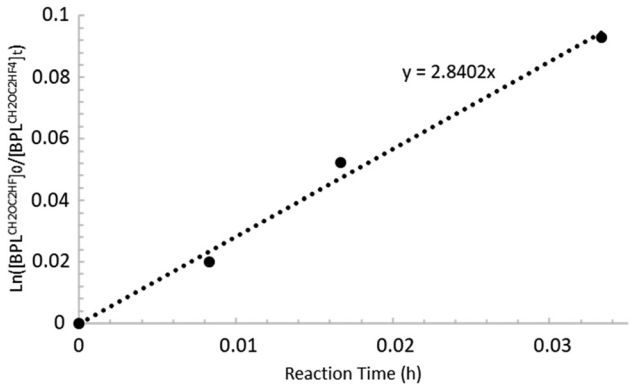

Fig. 1 Semi-logarithmic first-order plot for the ROP of *rac*-BPL^{CH_2OCF_2CHF_2} mediated by **1b**/*i*PrOH (20 °C, toluene; [BPL^{CH_2OCF_2CHF_2}]$_0$/{[**1c**]$_0$/[*i*PrOH]$_0$} = 250 : 1 : 1; Table 1 entries 11–14).

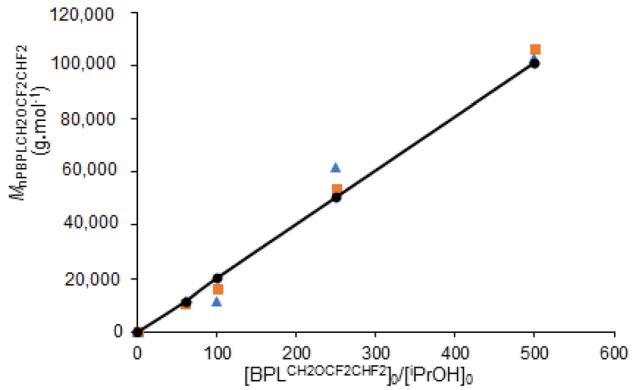

Fig. 2 Variation of $M_{n,NMR}$ ■, $M_{n,SEC}$ ▲, and $M_{n,theo}$ ● (solid line) values of PBPL^{CH_2OCF_2CHF_2} synthesized from the ROP of *rac*-BPL^{CH_2OCF_2CHF_2} mediated by the **1c**/*i*PrOH (1 : 1) catalyst system as a function of the BPL^{CH_2OCF_2CHF_2} monomer loading (Table 1, entries 8, 10, 15, and 16).

and 2). The reaction was quenched by addition of acetic acid (*ca.* 0.5 mL of a 1.6 mol L^{-1} solution in toluene). The resulting mixture was concentrated to dryness under vacuum and the conversion was determined by ^{1}H NMR analysis of the residue in $(CD_3)_2CO$. The crude polymer was then dissolved in acetone (*ca.* 1 mL) and precipitated in cold pentane (*ca.* 5 mL), filtered and dried. PBPL^{CH_2OCF_2CHF_2} was recovered as a white solid (120 mg, 60%). ^{1}H NMR (400 MHz, $(CD_3)_2CO$, 25 °C): δ (ppm) 6.23 (tt, $^3J_{H-F}$ = 3, $^1J_{H-F}$ = 53, 1H, OCF_2CHF_2), 5.47 (m, 1H, CH_2CHCH_2O), 4.99 (septet, $^2J_{H-H}$ = 7, 1H terminal group, $(CH_3)_2CHC(O)$), 4.27 (m, 2H, $CHCH_2OCHF_2$), 2.82 (m, 2H, $C(O)CH_2CH$), 1.21 (d, 6H terminal group, $(CH_3)_2CHOC(O)$); ^{13}C J-MOD NMR (100 MHz, $(CD_3)_2CO$, 25 °C) δ (ppm): 169.6 (*C*=O), 118.3 (tt, $^1J_{C-F}$ = 250, $^2J_{C-F}$ = 42, OCF_2CF_2H), 109.3 (tt, $^1J_{C-F}$ = 269, $^2J_{C-F}$ = 32, OCF_2CF_2H), 69.1 ($C(O)CH_2CH$), 66.7 ($(CH_3)_2CHO$), 65.5 ($CHCH_2O$), 35.5 ($C(O)CH_2CH$), 22.0 ($(CH_3)_2CHO$); ^{19}F{^{1}H} NMR (376 MHz, $(CD_3)_2CO$, 25 °C) δ (ppm): −138.2 (OCF_2CF_2H), −92.1 (OCF_2CF_2H) (Fig. 3). All recovered polymers were then thoroughly analyzed by NMR spectroscopy (Fig. 2, 3, 5 and S8–S13†), SEC (Fig. 2 and S14–S16†), mass spectrometry (Fig. 4), DSC (Fig. S17–S19†) and TGA (Fig. S20–S22†).

Results and discussion

The herein investigated fluorinated functional 4-substituted-β-propiolactone *rac*-BPL^{CH_2OCF_2CHF_2} was first synthesized in good yields on a multi-gram scale (up to 2.6 g, *ca.* 75%) from the carbonylation reaction of the parent epoxide, *rac*-BPL^{CH_2OCF_2CHF_2}, according to the adaptation of a typical procedure (Fig. S5–S7†).[41] While the synthesis of *rac*-BPL^{CH_2OCF_2CHF_2} was previously reported by Coates and coworkers, its preliminary homopolymerization therein mediated by a zinc β-diketiminate catalyst (BDI)Zn(OiPr) (6 h at 50 °C) returned a single PBPL^{CH_2OCF_2CHF_2} sample (95% monomer conversion, $M_{n,SEC(THF)}$ = 20 000 g mol^{-1} and $Đ_M$ = 1.14, T_g = −12 °C, no T_m observed; atactic polymer).[41] No further ROP was therein reported. For the sake of comparison with our data, we have reproduced this latter experiment under the conditions implemented in our study, *i.e.*, in toluene at room temperature and using the *in situ* catalyst combination (BDI)Zn(N(SiMe$_3$)$_2$)/*i*PrOH (Table 1, entry 1).

The ROP of *rac*-BPL^{CH_2OCF_2CHF_2} promoted by the yttrium catalyst systems Y{ONNO^{R2}}/*i*PrOH (R = Me, Cl, *t*Bu, CMe_2Ph, **1a–d**/*i*PrOH) was then investigated using the previously established optimized conditions, namely in toluene solution at room temperature (*ca.* 20 °C) (Scheme 3). The catalysts were conveniently generated *in situ* upon the addition of 1 equiv. of *i*PrOH, added as a co-initiator to a mixture of the proligand {ONNO^{R2}}H$_2$ and the yttrium amido precursor [Y(N(SiHMe$_2$)$_2$)$_3$](THF)$_2$, respectively, as typically performed.[10–17] Of note, the exploration of the impact of different *para*-R substituents on the phenolate proligand of complexes **1** was not undertaken in the present study, since they were previously demonstrated to have, in contrast to *ortho*-substituents, a minimal/negligible effect on the catalyst/initiator activity and stereoselectivity in the ROP of alike β-propiolactones.[9–17] Also, reaction conditions affording controlled, maximized or optimized molar mass and dispersity values were not sought after in the present work. The main objective of the current study was to gain further insights into the contribution to the stereocontrol of the ROP of potential NCIs between hydrogens from the methylene within the –C*H*$_2$OC*H*$_2$R* moiety of the functional side group on the repeating unit of the growing polymer chain, and the *ortho*-aryl R substituents of the {ONNO^{R2}} ligand. The ROP performance of the catalyst systems was first assessed, including their ability to promote stereoselective polymerization, as assessed by NMR and mass spectrometry analyses of the macromolecular characteristics of the resulting polyesters. The most significant data for the synthesized PBPL^{CH_2OCF_2CHF_2}s are gathered in Table 1 and discussed thereafter.

Among the different catalyst systems **1a–d**/*i*PrOH, the dimethylated Y{ONNO^{Me_2}} **1a** was found to be the least active in the ROP of *rac*-BPL^{CH_2OCF_2CHF_2}, only consuming 50 monomer

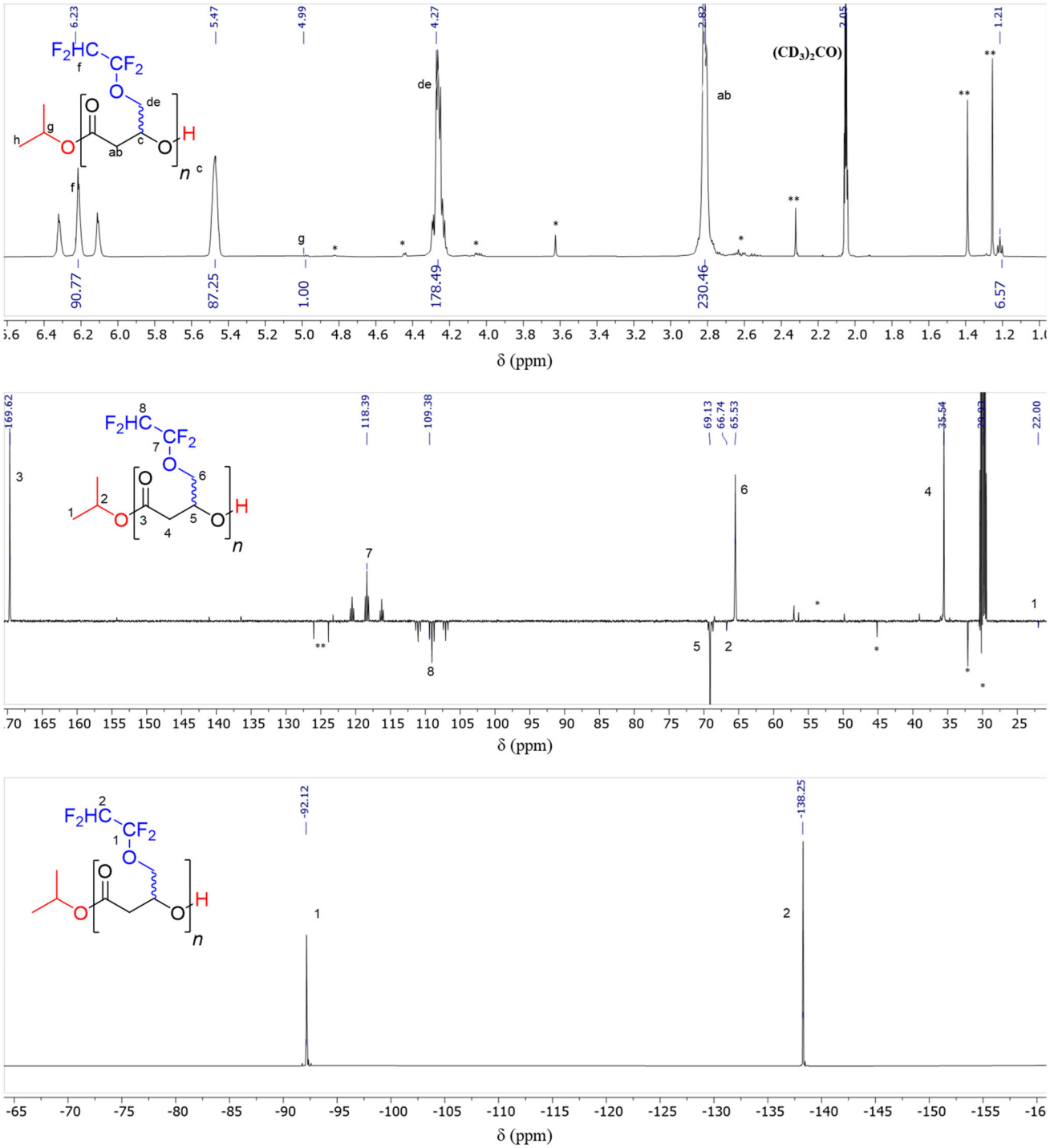

Fig. 3 ^{1}H NMR (400 MHz, $(CD_3)_2CO$, 25 °C), $^{13}C\{^{1}H\}$ J-MOD NMR (100 MHz, $(CD_3)_2CO$, 25 °C) and $^{19}F\{^{1}H\}$ NMR (376 MHz, $(CD_3)_2CO$, 25 °C) spectra of a $PBPL^{CH_2OCF_2CHF_2}$ polymer prepared from the ROP of *rac*-$BPL^{CH_2OCF_2CHF_2}$ mediated by the **1c**/*i*PrOH (1 : 1) catalyst system (Table 1, entry 10). * and ** stand for resonances of the residual solvent and/or catalyst.

units in 2 days with a turnover frequency (TOF expressed in $mol_{BPLCH_2OCF_2CHF_2}\ mol_{catalyst}^{-1}\ h^{-1}$) $TOF_{\mathbf{1a}}$ of 1.04 h^{-1} (Table 1, entries 3 and 4). The similarly uncrowded dichloro Y {$ONNO^{Cl_2}$} **1b** system showed a slightly better, yet still low activity, enabling the complete consumption of 100 monomer equiv. in 18 h with $TOF_{\mathbf{1b}}$ = 5.6 h^{-1} (Table 1, entries 5–7). Similar modest activities of these two catalyst systems were previously observed in the ROP of *rac*-LA and *rac*-4-substituted β-lactones and accounted for the likely formation of dinuclear/aggregated yttrium species, due to insufficient bulkiness of the

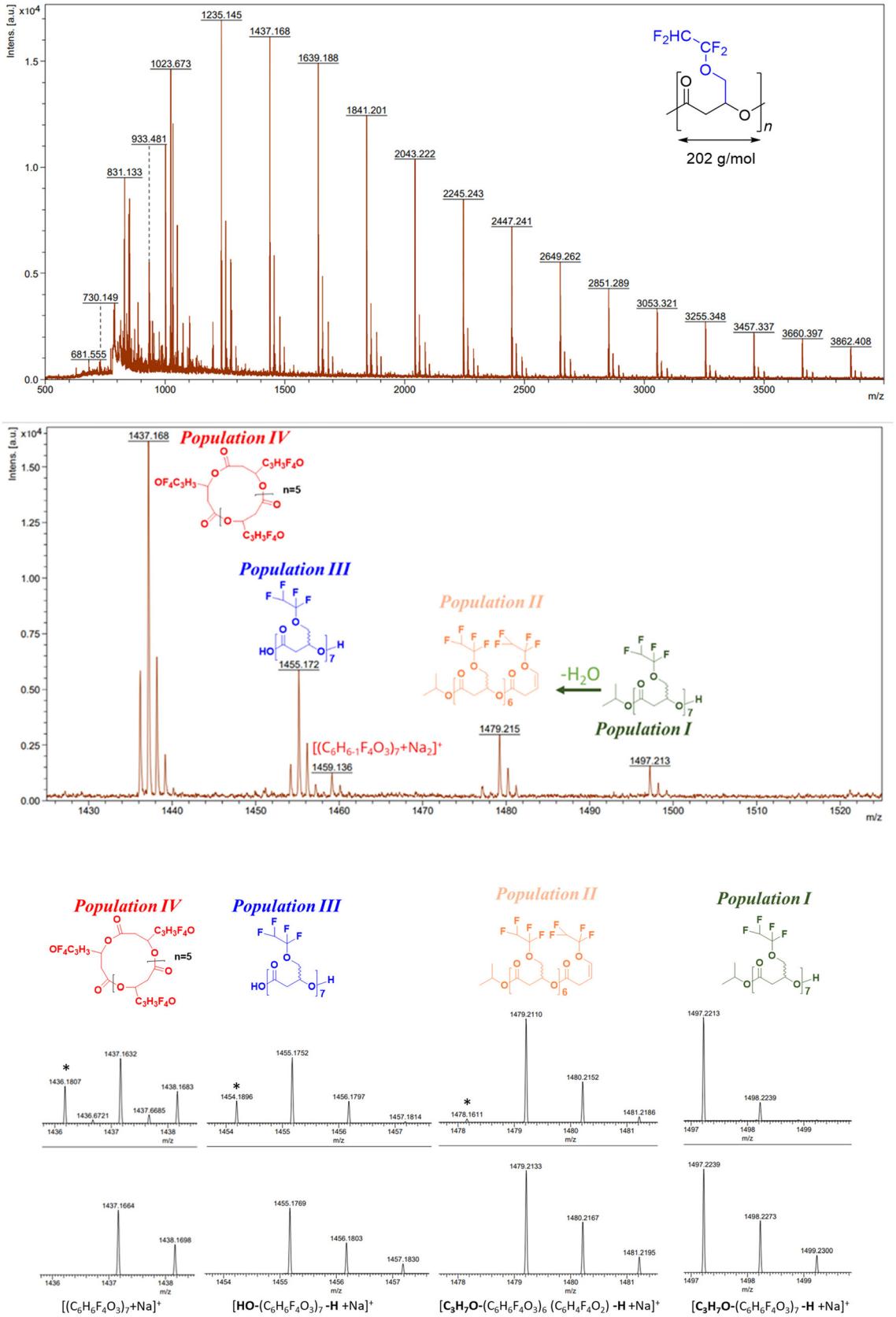

Fig. 4 High-resolution MALDI-ToF mass spectrum (top; positive mode, DCTB matrix, Na^+ cationizing salt) of a $PBPL^{CH_2OCF_2CHF_2}$ sample prepared from the ROP of *rac*-$BPL^{CH_2OCF_2CHF_2}$ (M = 202 g mol^{-1}) using **1d**/*i*PrOH (Table 1, entry 17), showing the zoomed regions of different populations **I–IV** (middle), and the corresponding correlation with the simulated spectra (bottom). * refers to the same series minus one H.

ortho-substituents of the ligand.[9,11] The alike ROP from **1b** performed in chlorobenzene or THF turned out to be even slower – and poorly controlled in terms of molar mass and dispersity – regardless of the solvent polarity ($TOF_{\mathbf{1b}/C_6H_5Cl}$ = 0.7 h^{-1}; $TOF_{\mathbf{1b}/THF}$ < 0.6 h^{-1}; Table 1, entries 19, 21 and 22). Then, the bulkier cumyl-substituted yttrium catalyst **1d** (R = CMe_2Ph), surprisingly, did not improve the ROP kinetics much, regardless of the solvent used (toluene, chlorobenzene or THF; $TOF_{\mathbf{1d}}$ < 4 h^{-1}; Table 1, entries 2, 17, 18, 20 and 23). Nevertheless, ROP performed with **1d** in slightly polar non-coordinating chlorobenzene was significantly faster than that in THF, in which the solvent competed with the monomer to coordinate with the yttrium center, a phenomenon already well established.[9–17] This rather poor activity of the bulky catalyst **1d** contrasts with the one observed for the similarly bulky, yet more active *t*Bu-substituted catalyst system Y{ONNO^{tBu2}} **1c**. The latter one, expectedly,[9,11] was found to be significantly more active, enabling the ready, complete conversion of 60 to 500 equiv. of *rac*-BPL^{CH_2OCF_2CHF_2} in toluene at room temperature (Table 1, entries 8–16). While 500 monomer equiv. were fully consumed in less than 4 h ($TOF_{\mathbf{1c}} \gg 125$ h^{-1}; Table 1, entry 16; note that reaction times herein reported were not optimized), the highest activity was observed for the conversion of 77 monomer equiv. within 30 s ($TOF_{\mathbf{1c}/77\ equiv.}$ = 4650 h^{-1}; Table 1, entry 12). Only the highest activity previously achieved in the ROP of the parent β-thiobutyrolactone ($TOF_{\mathbf{1c}/50\ equiv.}$ up to 3000 h^{-1})[51] and the correlated malolactonates *rac*-BPL^{CO_2Me,CO_2All,CO_2Bn} ($TOF_{100\ equiv.}$ = 3000 h^{-1}),[17] yet mediated by the related *t*Bu-substituted yttrium catalyst featuring a methoxy cap {ON(OMe)O^{tBu2}} in place of the amido cap {ON(NMe$_2$)O^{tBu2}} as in the present catalyst **1c**, is close to this present record value herein established.[8,10–17] Monitoring the polymerization of *rac*-BPL^{CH_2OCF_2CHF_2} performed with **1c**/*i*PrOH returned a linear semi-logarithmic plot, thus revealing that the reaction was first order in the monomer with an apparent rate constant k_{app} = 2.84 ± 0.034 in h^{-1} (Fig. 1). Hence, overall, the ROP of *rac*-BPL^{CH_2OCF_2CHF_2} proceeded more rapidly with the more sterically encumbered *t*Bu-substituted catalyst **1c** and falls within the range of rates recorded for other related functionalized BPL^{FG}s (FG = CH_2OMe, CH_2OAll, CH_2OPh, CH_2CH_2OBn, CH_2CH_2OiPr, CH_2CH_2OtBu, and $CH_2CH_2OSitBuMe_2$), using the same diamino- and aminoalkoxy-bisphenolate yttrium catalysts.[9–17] The unexpected low activity of the cumyl-substituted system **1d** possibly suggests detrimental (in terms of activity) electronic interactions involving the phenyl rings in the cumyl-substituents; attractive C*H*···π electronic interactions involving the phenyl rings of the cumyl-substituted catalyst have already been suggested in the ROP of *rac*-BPL^{Me} with similar Y{ONXO^{cumyl2}} systems,[9] as well in the ROP of *rac*-LA with {BDI^{aryl}}Mg(OR) catalyst systems, as supported by DFT calculations.[19] Yet, these were not probed in the present study.

The catalyst systems **1a–d**/*i*PrOH showed good control over the macromolecular characteristics of the polyesters, especially in terms of molar mass and dispersity. The experimental molar mass values, as determined by ^{1}H NMR and SEC analyses of the PBPL^{CH_2OCF_2CHF_2} samples ($M_{n,NMR}$ and $M_{n,SEC}$, respectively), were generally matching the calculated data ($M_{n,theo}$) established from the monomer conversion as estimated by NMR analysis of the crude samples (*i.e.*, before precipitation of the polymer; refer to the Experimental section) (Table 1). PBPL^{CH_2OCF_2CHF_2} samples with $M_{n,NMR}$ values ranging from 2300 to 106 000 g mol^{-1} were thus isolated with a fairly narrow dispersity value ranging from 1.02 to 1.24 (Table 1). As depicted in Fig. 2 for the ROP of *rac*-BPL^{CH_2OCF_2CHF_2} promoted by **1c**/*i*PrOH, the experimental $M_{n,NMR}$ values varied linearly with the monomer loading/conversion, in agreement with the theoretical data as well. Altogether, these observations thereby confirmed the ability of these Y{ONXO^{R2}} systems to limit the occurrence of side reactions, namely inter- and intra-molecular transesterifications, *i.e.*, reshuffling and back-biting reactions, respectively, as typically encountered in ROP of cyclic esters or carbonates.

The PBPL^{CH_2OCF_2CHF_2} polymers were characterized by 1D, 2D NMR and mass spectrometry analyses. The ^{1}H, ^{13}C J-MOD, ^{19}F NMR and 2D spectra showed the expected characteristic signals corresponding to the BPL^{CH_2OCF_2CHF_2} repeating units (Fig. 3 and S7–S9†). In particular, the methine (δ 5.47 ppm) and methylene (δ 2.82 ppm) typical ^{1}H signals of the polyester backbone, along with the distinctive signals of the –$CH_2OCF_2CHF_2$ pendent moiety observed in ^{1}H, ^{13}C and ^{19}F NMR spectra (δ_{CH_2O} 4.27 ppm, δ_{CHF_2} 6.23 ppm, δ_{CH_2O} 65.5 ppm, δ_{OCF_2} 118.4 ppm, δ_{CHF_2} 109.4 ppm, δ_{OCF_2} −92.1 ppm, and δ_{CHF_2} −138.2 ppm), all supported the formation of the awaited PBPL^{CH_2OCF_2CHF_2}. The characteristic isopropoxycarbonyl chain-end group signature was also unambiguously observed (δ_{OCH} 4.99 ppm, δ_{OCHMe_2} 1.21 ppm; δ_{OCHMe_2} 66.7 ppm, δ_{OCHMe_2} 22.0 ppm), thus supporting the formation of linear macromolecules and that the *in situ* prepared {ONNO^{R2}}Y(OiPr) alkoxide complex is indeed the active species that initiates the polymerization (Scheme 3). Furthermore, the DOSY NMR spectrum of a PBPL^{CH_2OCF_2CHF_2} sample evidences the presence of a single population of macromolecules that are end-capped by isopropoxy end-groups (Table 1, entry 17; Fig. S10†). This selective formation of isopropoxy terminated macromolecules is also corroborated by the good match between theoretical M_n values and experimental M_n values determined by NMR considering the presence of an isopropoxy end-group for each macromolecule (*vide supra*, Table 1).

MALDI-ToF mass spectrometry investigations of a low molar mass sample prepared from the **1d**/*i*PrOH catalyst enabled us to gain deeper insights into the macromolecular structure and topology of PBPL^{CH_2OCF_2CHF_2}. A typical mass spectrum, recorded using a DCTB matrix, for a sample prepared from the ROP of *rac*-BPL^{CH_2OCF_2CHF_2} using **1d**/*i*PrOH (Table 1, entry 17), is illustrated in Fig. 4. It shows a set of four distinct populations of macromolecules ionized by Na^+, all featuring the anticipated repeating unit of *m*/*z* 202 corresponding to the monomer ($M_{BPL(CH_2OCF_2CHF_2)}$) (Fig. 4). The first population of linear macromolecules featuring α-isopropoxyl and ω-hydroxyl end groups was observed (green population **I**), as anticipated for the ROP of *rac*-BPL^{CH_2OCF_2CHF_2} promoted by **1d**/

*i*PrOH. The second population was assigned to linear α-isopropoxy,ω-crotonate telechelic PBPL^{CH_2OCF_2CHF_2} chains, arising from ω-dehydration of the former population **I** (orange population **II**). Such a crotonate chain-end formation upon H_2O elimination is not surprising, as it is a known side reaction reported to be occurring during the synthesis of polyesters by ROP of such β-lactones.[13,16,52] Another population derived from population **I** upon abstraction of the isopropyl end-group, showed linear macromolecules with α-carboxylic acid and ω-hydroxyl end-capping groups (blue population **III**). A careful analysis of NMR spectra of various polymer samples did not reveal any distinctive alkene signals (anticipated $\delta_{^1H}$ *ca.* 6.25, 5.77 ppm, $\delta_{^{13}C}$ *ca.* 144.9, 120.5 ppm),[52] nor any carboxylic acid signals (anticipated $\delta_{^1H}$ *ca.* 10.00 ppm, $\delta_{^{13}C}$ *ca.* 196.4 ppm),[52] corresponding to such α-OiPr, ω-COCH$_2$*CH*=*CH*OCF$_2$CHF$_2$ or α-COO*H*,ω-OH telechelic PBPL^{CH_2OCF_2CHF_2} chains, respectively (Fig. 4). This observation thus suggested that these latter two populations **II** and **III** were most likely formed during the mass spectrometry analysis (*i.e.*, promoted by the acidic DCTB matrix), or that they actually represented minor populations undetectable by NMR, *i.e.*, they corresponded to negligible species present within the isolated polymers which are overexpressed in the MS analysis. Finally, the last population observed was attributed to cyclic PBPL^{CH_2OCF_2CHF_2} chains (red population **IV**; undetectable by NMR analysis since they feature the same repeating unit as linear macromolecules). The observation of a significant population of cyclic macromolecules by MALDI-ToF MS most likely results from the sample preparation (in an acidic DCTB matrix, which shall promote easy transesterification/cyclization) and/or incidental over-expression (co-crystallization, ionization) of cyclic macromolecules (over linear ones). These four populations of macromolecular chains were unequivocally confirmed by the close match of the high-resolution experimental spectrum with the corresponding isotopic simulations, as illustrated in Fig. 4; for example, for population **I** – [(CH$_3$)$_2$CHO(COCH$_2$CH(CH$_2$OCF$_2$CHF$_2$)O)$_n$H]·Na$^+$ with *m*/*z* calculated 1497.2213 *vs.* found 1497.213 for *n* = 7; population **II** – [(CH$_3$)$_2$CHO(COCH$_2$CH(CH$_2$OCF$_2$CHF$_2$)O)$_n$ (COCH$_2$*CH*=*CH*OCF$_2$CHF$_2$)]·Na$^+$ with *m*/*z* calculated 1479.2110 *vs.* found 1479.215 for *n* = 6; population **III** – [HO(COCH$_2$CH(CH$_2$OCF$_2$CHF$_2$)O)$_n$H]·Na$^+$ with *m*/*z* calculated 1455.1752 *vs.* found 1455.172 for *n* = 7; and population **IV** – [(COCH$_2$CH(CH$_2$OCF$_2$CHF$_2$)O)$_n$]·Na$^+$ with *m*/*z* calculated *m*/*z* 1437.1632 *vs.* found 1437.168 for *n* = 5.

In order to assess the ability of the catalyst systems **1a–d**/*i*PrOH to stereoselectively promote the ROP of *rac*-BPL^{CH_2OCF_2CHF_2}, and in turn to evaluate the possible role of NCIs in promoting stereocontrol, ^{13}C J-MOD NMR spectra of the samples were closely examined. The spectrum of an isotactic-rich PBPL^{CH_2OCF_2CHF_2}, synthesized from the ROP of enantio-enriched (*S*)-BPL^{CH_2OCF_2CHF_2} using **1d**/*i*PrOH, was first acquired as a reference of an isotactic polymer (Table 1, entry 2).[50] From our previous studies on ROP of chiral β-lactones mediated by such achiral yttrium diamino- or amino-alkoxy-bisphenolate complexes, we have established that the stereocontrol of these ROPs proceed through the so-called chain-end mechanism (CEM). The CEM involves tuning and selection of the chirality of the next monomer to be inserted, as dictated by the chirality of the last (first-order) or the last and penultimate (second-order) monomer unit inserted into the propagating yttrium-polymeryl species. Thus, a regular CEM of the ROP of such a chiral racemic BPL^{CH_2OCF_2CHF_2} β-propiolactone, would generate syndiotactic PBPL^{CH_2OCF_2CHF_2} upon inserting the monomer of configuration opposite to that of the last inserted one, thereby minimizing steric hindrance in the transition state.[6–9] The ^{13}C NMR spectra of PBPL^{CH_2OCF_2CHF_2} recovered from the ROP of (*S*)- and *rac*-BPL^{CH_2OCF_2CHF_2} promoted by **1a–d**/*i*PrOH are depicted in Fig. 5 and S9,† comparatively showing the carbonyl, and methylene and methine signals of the repeating units (*C*^{3}O*C*^{4}H$_2$*C*^{5}H(CH$_2$OCF$_2$CHF$_2$)).

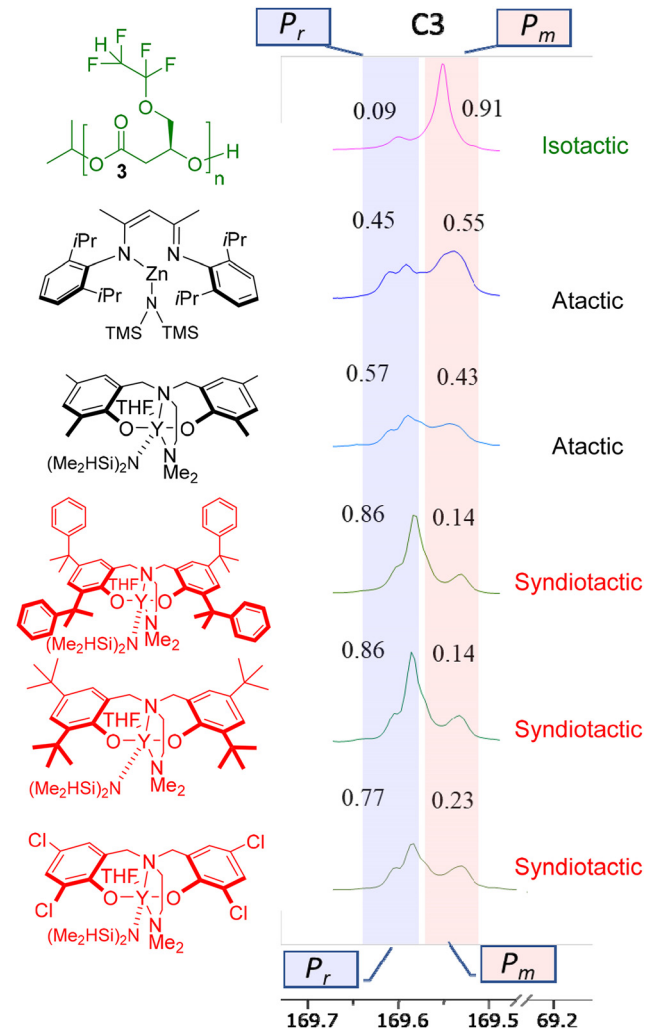

Fig. 5 Zoomed carbonyl region of the ^{13}C J-MOD NMR spectra (125 MHz, (CD$_3$)$_2$CO, 23 °C) of PBPL^{CH_2OCF_2CHF_2}s prepared by ROP of *rac*-BPL^{CH_2OCF_2CHF_2}, except for the top spectra of enantiopure (*S*)-BPL^{CH_2OCF_2CHF_2}, mediated by (BDI)ZnN(SiMe$_3$)$_2$/*i*PrOH and **1a–d**/*i*PrOH catalyst systems in toluene at 20 °C (Table 1, entries 1, 2, 3, 5, 8 and 18).

The highly isotactic PBPL^{CH_2OCF_2CHF_2} sample provided the reference spectrum from which the catalysts stereoselectivity was thus assessed (Fig. 5 – top spectrum). It exhibits two distinct signals in the carbonyl region (δ *ca.* 169.60 ppm), assigned to the *meso* (*m*) and *racemo* (*r*) diads, with the *meso* signal being the most intense (P_m = 0.91;[50] $\delta_{C=O}r$ *ca.* 169.60, $\delta_{C=O}m$ *ca.*169.55). In comparison, the methine and methylene signals (δ 69.13, 65.53, and 35.54 ppm, respectively) did not show any deconvolution at the diad level, possibly due to the carbon coupling to fluorine (Fig. S11†). Thus, the tacticity of the polymers was evaluated from the intensity of *meso* and *racemo* diad signals of the carbonyl region, from which P_m and P_r values were determined. As expected, the ROP mediated by (BDI)ZnN(SiMe$_3$)$_2$/*i*PrOH, known as a non-stereoselective catalyst towards *rac*-β-lactones,[6,41] returned an atactic polymer (P_r = 0.45; the two diad signals are similarly intense and broadened *vs.* the corresponding isotactic signals). Moving to the {ONNO^{R2}}Y catalyst systems, the uncrowded dimethyl-substituted complex **1a** did not show any stereoselectivity, giving polymers with P_r = *ca.* 0.55, thus following the common trend we reported earlier.[9,11] Note that within the series of our reported BPL^{FG}s, high syndioselectivity using **1a** was only observed – in place of the common non-stereoselective ROP affording atactic PHAs – in the ROP of the functionalized monomers with FG = CH$_2$OiPr, CH$_2$O*t*Bu, CH$_2$OPh, CH$_2$OSi*t*BuMe$_2$, CH$_2$SPh, CO$_2$Me, CO$_2$All, and CO$_2$Bn (Table 2).[12,13] The sterically near-equivalent dichloro catalyst **1b** gave more syndio-enriched polymers with P_r = *ca.* 0.73. The overall stereoselective ability of catalyst **1b** observed in the ROP of alike BPL^{FG}s returns either atactic (FG = Me, CH$_2$CH$_2$OBn) or more commonly syndiotactic (FG = CH$_2$OiPr, CH$_2$O*t*Bu, CH$_2$OSi*t*BuMe$_2$, CH$_2$OPh, CH$_2$SPh, CO$_2$Me, CO$_2$All, CO$_2$Bn) PHAs, while more unusual isotactic ones have only been reported with the 4-alkoxymethylene-β-propiolactones (FG = CH$_2$OMe/All/Bn) (Table 2). On the other hand, both yttrium complexes bearing ligands flanked with bulky *ortho*,*para*-R,R substituents (R = *t*Bu and cumyl; namely **1c** and **1d**, respectively) consistently induced the formation of highly syndioregular polymers with P_r = 0.79–0.87. This latter propensity of the sterically bulkier yttrium catalysts to promote the formation of syndiotactic PHAs is invariably observed in the similarly yttrium-catalyzed ROP of all the BPL^{FG}s we have investigated so far, regardless of the chemical nature of the functional pending substituent, be it methylene-alkyl, -fluoroalkyl, -alkoxy, -silyloxy, or alkoxycarbonyl exocyclic side-groups. Note that, changing the solvent from toluene to THF or chlorobenzene did not affect significantly the syndioselectivity of the resulting PBPL^{CH_2OCF_2CHF_2}, as assessed from **1b** and **1d**. However, no iso-enriched PBPL^{CH_2OCF_2CHF_2} could thus be prepared under these operating conditions.

Noteworthily, the dichloro-substituted catalyst **1b** favored a similar syndio-enrichment in PBPL^{CH_2OCF_2CHF_2} (P_r = 0.69–0.77) to that in PBPL^{CH_2OPh} (P_r = 0.73–0.77), both PHAs arising from 4-alkoxymethylene-substituted β-propiolactones, and each monomer being depleted of any outer methylene hydrogens within the terminal alkoxy moiety, namely CH$_2$O$\underline{C}$F$_2$CHF$_2$ and CH$_2$O$\underline{C}_6\underline{H}_5$, respectively (Table 2).[13] Such replacement within the exocyclic alkoxy moiety of BPL$^{CH_2OC\underline{H}_2R^*}$ of hydrogen by fluorine or by a quaternary sp^2 carbon, clearly impeded the formation of NCIs with the yttrium phenolate chloro substituent that was expected/understood to induce stereoselectivity in the returned PHAs. Hence, this observation further supports our previously suggested hypothesis – based on former experimental and *in silico* results –, that both the inner and outer two hydrogens, as in BPL$^{\underline{CH}_2O\underline{CH}_2R^*}$, are required to induce the necessary NCIs with the phenolate *ortho*-chloro substituent on the yttrium catalyst. Unfortunately, the perfluorinated β-lactone with any inner and outer methylene hydrogens depleted remained synthetically inaccessible.

Note that, while both inner and outer methylene hydrogens in BPL$^{\underline{CH}_2O\underline{CH}_2R^*}$ experimentally appear to be simultaneously required to achieve isoselectivity (Table 2), DFT computations suggested that the NCIs of the *ortho*-chloro substituent are stronger with the inner methylene hydrogens ($Cl\cdots\underline{H}_2\underline{C}OCH_2CHCH_2$ distance = 2.556 Å) than with the outer methylene hydrogens ($Cl\cdots\underline{H}_2\underline{C}(CHCH_2)OCH_2$ distance = 3.083 Å).[15] Increasing the bulkiness in an outer methylene-free alkoxide BPL^{FG} as with FG = CH$_2$O$\underline{C}\underline{R}^{\#}$ = CH$_2$O$\underline{i}$Pr, CH$_2$O$\underline{t}$Bu, CH$_2\underline{O}$Ph, CH$_2\underline{O}$Si$\underline{t}$Bu$\underline{M}\underline{e}_2$ also revealed that a sterically encumbered FG substituent could not promote isoselectivity by itself.[12] Replacing oxygen (alkoxy) with sulfur (thioether) in the outer moiety (*i.e.*, FG = CH$_2\underline{S}$Ph *vs.* CH$_2\underline{O}$Ph) similarly did not provide an appropriate stereoelectronic environment favorable for the formation of $Cl\cdots\underline{H}_2\underline{C}O$ NCIs.[13] Lengthening the inner methylene of the alkoxymethylene functional group using an additional methylene (*i.e.*, FG = $\underline{C}\underline{H}_2\underline{C}\underline{H}_2$OBn *vs.* $\underline{C}\underline{H}_2$OBn) was also found to be unsuccessful for iso-enrichment of the resulting PHA, in spite of the presence of both inner and outer methylenes apart the central oxygen.[13] Finally, the introduction of a chemically distinct functional group (*vs.* alkoxymethylene FG as in BPL$^{\underline{CH}_2O\underline{CH}_2\underline{R}^*}$) using an ester substituent into the β-propiolactone monomer, as within the related alkyl β-malolactonate series (BPL^{FG} with FG = CO$_2$Me, CO$_2$All, CO$_2$Bn), also switched stereoselectivity from isotactic to syndiotactic.[16,17] Last but not least, moving from classical oxolactone to its parent thiolactone upon exchanging the endocyclic oxygen with sulfur (*i.e*, going from β-butyrolactone to β-thiobutyrolactone) did not suitably impact the electronic environment on the exocyclic methyl substituent to provide isotacticity.[51] Consequently, iso-enriched PBPL^{FG}s have so far only been obtained from {ONXO^{F2,Cl2,Br2}}Y-catalyzed ROP of β-propiolactone monomers featuring both inner and outer methylene hydrogens within the 4-alkoxymethylene exocyclic substituent, namely BPL$^{\underline{CH}_2O\underline{CH}_2\underline{R}^*}$ with R* = CH$_3$ (FG = CH$_2$OMe), CH$_2$-CH=CH$_2$ (FG = CH$_2$OAll), or Ph (FG = CH$_2$OBn) (Table 2).

In addition, as the crystallinity of a polymer is closely dependent on its tacticity, PBPL^{CH_2OCF_2CHF_2} samples with different tacticities were analyzed by differential scanning calorimetry (DSC; Table 1 and Fig. S17–S19†). All thermograms showed a sub-0 °C glass transition temperature (T_g) ranging from −25.0 to −5.8 °C, while no melting temperature (T_m) was

Table 2 Stereoselectivity (P_r) and thermal characteristics (T_g, T_m, and T_d) of PBPL^{FG}s with FG = Me, CO_2R (R = Me, All, Bn), CH_2OR (R = Me, All, Bn, Ph, *i*Pr, *t*Bu, $SiMe_2tBu$), CH_2SPh, CH_2CH_2OBn, and $CH_2OCF_2CHF_2$, prepared by ROP of the corresponding *rac*-BPL^{FG}s promoted by yttrium catalyst systems Y{ONXO^{R2}} **1a–d**/*i*PrOH (reference numbers for each β-lactone are provided below the formulae)

	 *rac*-BPL^{FG}s		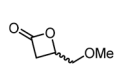	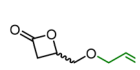	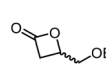	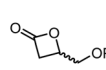	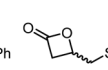	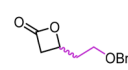	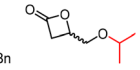	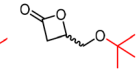	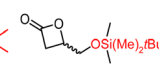	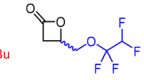
Cat.**1** (R′ = R″)	*rac*-BPL^{CH_3} 7 and 53	*rac*-MLA^{R} R = Me, Bn, All 7, 16 and 17	*rac*-BPL^{CH_2OMe} 15	*rac*-BPL^{CH_2OAll} 15	*rac*-BPL^{CH_2OBn} 15	*rac*-BPL^{CH_2OPh} 13	*rac*-BPL^{CH_2SPh} 13	*rac*-BPL^{CH_2CH_2OBn} 13	*rac*-BPL^{CH_2OiPr} 12	*rac*-BPL^{CH_2OtBu} 12	*rac*-BPL^{CH_2OTBDMS} 12	*rac*-BPL^{CH_2OCF_2CHF_2} (This work)
Crowded (cumyl, *t*Bu) (**1c** and **1d**)	[e] **Syndiotactic** P_r = 0.80–0.91 T_m = 133–178 °C T_g = n.d.[d]	**Syndiotactic** P_r = 0.76–0.82 T_m = 49–173 °C T_g = 30–40 °C	**Syndiotactic** P_r = 0.78–0.81 T_m = 116 °C T_g = −12 °C	**Syndiotactic** P_r = 0.81–0.84 T_m = 85 °C T_g = −38 °C	**Syndiotactic** P_r = 0.85–0.90 No T_m obsv. T_g = 0 °C	**Syndiotactic** P_r = 0.81–0.87 No T_m obsv T_g = 37–40 °C	**Syndiotactic** P_r = 0.83–0.87 No T_m obsv T_g = 12–14 °C	**Syndiotactic** P_r = 0.77–0.85 No T_m obsv T_g = −11–(−12) °C	**Syndiotactic** P_r = 0.82–0.86 No T_m obsv T_g = −18 °C	**Syndiotactic** P_r = 0.78–0.84 No T_m obsv T_g = −6 °C	**Syndiotactic** P_r = 0.81–0.87 T_m = 119 °C T_g = 9 °C	**Syndiotactic**[a] P_r = 0.70–0.86 No T_m obsv T_g = −6–(−23) °C
M_n (g mol^{-1})	≈35–60 000	≈5–15 000	≈5000	≈7–10 000	≈10 000	≈10–80 000	≈10–80 000	≈5–20 000	≈60 000	≈5000	≈35–90 000	≈10–100 000
Aliphatic non-crowded	P_r = 0.56 T_m = n.d.[d] T_g = n.d.[d]	rxn n.d.[d] rxn n.d.[d] rxn n.d.[d]	**Atactic** P_r = 0.49 No T_m obsv. T_g = −18 °C	**Atactic** P_r = 0.49 No T_m obsv. T_g = −40 °C	**Atactic** P_r = 0.50 No T_m obsv. T_g = −6 °C	**Syndiotactic** P_r = 0.76 No T_m obsv. T_g = 30 °C	**Syndiotactic** P_r = 0.74–0.76 No T_m obsv. T_g = 8–9 °C	**Atactic** P_r = 0.49 No T_m obsv. T_g = −12 °C	**Syndiotactic** P_r = 0.71–0.72 T_m = n.d.[d] T_g = n.d.[d]	**Syndiotactic** P_r = 0.74–0.75 T_m = n.d.[d] T_g = n.d.[d]	**Syndiotactic** P_r = 0.77 T_m = n.d.[d] T_g = n.d.[d]	**Atactic**[b] P_r = 0.53–0.57 No T_m obsv. T_g = −21 °C
M_n (g mol^{-1})	—	—	≈5000	≈7–10 000	≈10 000	≈10 000	≈5–10 000	≈7000	—	—	—	≈10 000
Halogenated non-crowded (Cl, **1b**)	[e] **Atactic** P_r = 0.42–0.45 T_m = n.d.[d] T_g = n.d.[d]	[e] **Syndiotactic** P_r = 0.89–0.95^{+} T_m = 111–207 °C T_g = 30–40 °C	**Isotactic** P_r = 0.10 No T_m obsv. T_g = −18 °C	**Isotactic** P_r = 0.09 No T_m obsv. T_g = −39 °C	**Isotactic** P_r = 0.10 No T_m obsv. T_g = 0 °C	**Syndiotactic** P_r = 0.75–0.77 No T_m obsv. T_g = 21–22 °C	**Syndiotactic** P_r = 0.73–0.74 No T_m obsv. T_g = 9 °C	**Atactic** P_r = 0.49 No T_m obsv. T_g = −15 °C	**Syndiotactic** P_r = 0.70 T_m = n.d.[d] T_g = n.d.[d]	**Syndiotactic** P_r = 0.70–0.71 T_m = n.d.[d] T_g = n.d.[d]	**Syndiotactic** P_r = 0.76 T_m = n.d.[d] T_g = n.d.[d]	**Syndiotactic**[c] P_r = 0.69–0.77 No T_m obsv. T_g = −12–(−17) °C
M_n (g mol^{-1})	— T_d = 256 °C	≈10–15 000 T_d = n.d.[d]	≈5000 T_d = n.d.[d]	≈7–10 000 T_d = n.d.[d]	≈10 000 T_d = n.d.[d]	≈5000 T_d = 272 °C	≈50 000 T_d = 271 °C	≈5000 T_d = 226 °C	— T_d = 211 °C	— T_d = 197 °C	— T_d = 195 °C	≈20 000 T_d = 195–203 °C

[a] Table 1, entries 8–18. [b] Table 1, entries 3 and 4. [c] Table 1, entries 5–7. [d] n.d. = not determined. [e] Y{ONOO^{R2}} [amino-alkoxy-bisphenolate]yttrium-amido complexes.

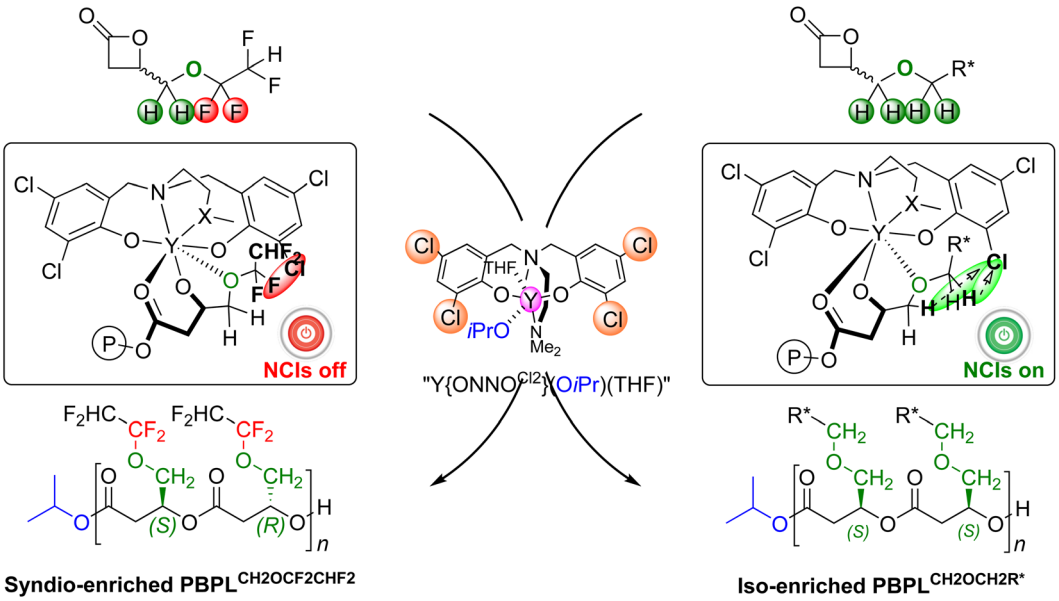

Scheme 4 Stereoselective ROP of chiral *racemic* 4-substituted-β-propiolactones, *rac*-BPL^{FG}s with (left) FG = $\underline{CH_2}O\underline{CH_2}R^*$ and R* = H, CH═CH_2, Ph, or (right) FG = $\underline{CH_2}O\underline{CF_2}CHF_2$, performed with the Y{ON(X)O^{Cl_2}}/*i*PrOH catalyst system, returning iso-enriched PBPL$^{CH_2OCH_2R^*}$ or syndio-enriched PBPL^{CH_2OCF_2CHF_2}, respectively, and illustrating the importance of the methylene-alkoxy-methylene moiety within the exocyclic side chain to impart isoselectivity through attractive NCIs.

observed below 200 °C in any of the samples (Table 1). Typically, the T_g values of PBPL^{CH_2OCF_2CHF} averaged to *ca.* −20 °C for $M_n \leq 25\,000$ g mol^{-1}, while a higher molar mass resulted, as anticipated, in higher T_g values (typically −5.8 °C for $M_{n,NMR}$ = 106 000 g mol^{-1}) (Table 1, entry 16). The absence of a melting transition for PBPL^{CH_2OCF_2CHF_2} suggested that all the fluorinated PHAs herein prepared were amorphous, regardless of their microstructure. This is in agreement with the thermal signature of the other parent perfluoroalkylated PBPL^{CH_2Y}s with Y = $CF(CF_3)_2$, $(CF_2)_3CF_3$, $(CF_2)_2CF(CF_3)_2$, C_6F_5, previously synthesized using the non-stereoselective (BDI)Zn(O*i*Pr) catalyst – hence returning atactic polymers –, which similarly did not exhibit T_m.[41] Note that among all the fluorinated PHAs prepared in this latter work, only the iso-enriched polymer ($M_{n,SEC}$ = 16 000 g mol^{-1}, $Đ_M$ = 1.1) prepared from the optically pure (*S*)-BPL^{CH_2OCF_2CHF_2}, was reported to show a minimal semi-crystalline signature with T_m = 101.9 °C and ΔH_m = 0.30 J g^{-1}. However, in this former literature report, no T_g was detected, whereas our analogous sample showed a T_g value (−7.8 °C; Table 1, entry 2) but no T_m. The lack of crystallinity in PBPL^{FG}s was similarly observed in other syndiotactic PBPL^{FG}s, with FG = CH_2O*i*Pr, CH_2O*t*Bu, CH_2OPh, CH_2OBn (Table 2). Actually, among the PBPL^{FG}s obtained by ROP of the corresponding *rac*-BPL^{FG}s from **1c** and **1d**/*i*PrOH catalyst systems, the only syndiotactic PHAs that featured a T_m value are the PBPL^{FG}s with FG = CH_3, CH_2OMe, CH_2OAll, CH_2OSi*t*$BuMe_2$, CO_2Me, CO_2All, and CO_2Bn (Table 2).[6,11,12,16] This lack of crystallinity in PBPL^{CH_2OCF_2CHF}, no matter the tacticity of the PHA main chain, may be inherent to the relatively long fluorinated pendent moiety. Finally, the thermal degradation profile of PBPL^{CH_2OCF_2CHF_2}, evaluated by TGA, typically exhibited a degradation temperature (at 5% mass loss of the polymer) of T_d = *ca.* 200 °C, within the lowest values of the 195–272 °C range determined for the related PBPL^{FG}s (Fig. S20–S22† and Table 2).

Conclusion

ROP of fluorinated 4-methylene-alkoxy-substituted β-propiolactone *rac*-BPL^{CH_2OCF_2CHF_2} mediated by Y{ONNO^{R2}}/*i*PrOH catalyst systems effectively proceeded towards the formation of the corresponding fluoroalkylated PHAs. Complete monomer consumption was observed at room temperature, yet at a different rate depending on the *ortho*,*para*-R,R phenolate substituents, with catalysts bearing a bulkier *tert*-butyl substituent being more active than those bearing smaller chloride and methyl ones, and also, unexpectedly, the cumyl substituent. Well-defined high molar mass and narrowly dispersed fluorinated PHAs ($M_{n,NMR}$ = 2300 to 106 000 g mol^{-1}; $Đ_M$ = 1.02–1.24) were isolated, showcasing a rather good control of the polymerization, especially emphasizing tunable molar mass values and limited undesirable transfer and/or transesterification side reactions. Molecular characterization of the polymers by NMR and mass spectrometry analyses confirmed the formation of α-isopropoxy,ω-hydroxy telechelic PBPL^{CH_2OCF_2CHF_2} chains; in particular, the *i*PrO– and HO– chain end groups were unambiguously identified. The thermal signature of PBPL^{CH_2OCF_2CHF_2} samples revealed amorphous thermoplastic fluorinated polyesters, similar to previously reported perfluoroalkyl-substituted PHAs (PBPL^{CH_2Z}, *vide supra*).[41]

Detailed analyses of the ^{13}C NMR spectra of the various polymers formed from the different catalyst systems showed that the dimethyl-substituted {ONNO^{Me_2}}Y complex **1a** promoted the formation of atactic polymers, while the dichloro {ONNO^{Cl_2}}Y catalyst **1b** and the bulkier *tert*-butyl- and cumyl-substituted catalysts **1c** and **1d**, respectively, all returned syndio-enriched PHAs with P_r up to 0.87. The thus recovered PBPL^{CH_2OCF_2CHF_2}s represent the first examples of stereoregular fluorinated PHAs that were chemically synthesized by ROP of the corresponding β-lactone. This stereoselectivity behavior, for a given *rac*-BPL^{CH_2OCF_2CHF_2} monomer, mainly dictated by the nature of the *ortho*-R substituent on the yttrium bisphenolate surrounding ligand, is in line with the general tendency which prevails in the ROP of such parent BPL^{FG}s: a "simple" modification of this ligand *ortho*-substituent enables the tuning of the stereoselectivity from atactic to syndiotactic PHAs. The {ONNO^{R2}}Y catalyst systems based on **1a–d** failed to provide isotactic PBPL^{CH_2OCF_2CHF_2}; the only examples of such iso-enriched related PHAs, chemically synthesized by ROP of a functional or non-functional β-lactone, remain, to date, the unique series of 4-alkoxymethylene functionalized BPL$^{CH_2OCH_2R^*}$s with R* = H, CH=CH_2, or Ph. Inhibiting NCIs between the *ortho*-chloro-substituted phenolate and the outer methylene hydrogens within the exocyclic 4-alkoxymethylene pending substituent upon fluorinating the alkyl (*i.e.*, $CH_2O\underline{C}F_2CHF_2$ *vs.* $CH_2O\underline{C}\underline{H}_2R^*$), while maintaining the inner methylene hydrogens available for such $Cl\cdots\underline{H}_2\underline{C}O$ attractive interactions, was thus found to be inefficient to impart isoselectivity during the ROP process. Combining our earlier findings gained from the BPL^{FG} series with FG = Me, CH_2O*i*Pr, CH_2O*t*Bu, CH_2OPh, $CH_2OSi(t\text{BuMe}_2)$, CH_2SPh, CO_2Me, CO_2All, and CO_2Bn (Scheme 1), the experimental results reported in the present work further highlight our initial assumption: methylene hydrogens have to be present at both the adjacent positions of oxygen (*i.e.*, both moieties bonded to oxygen) within the functional side-substituent on the monomer (FG = $\underline{C}\underline{H}_2O\underline{C}\underline{H}_2R^*$), and the chloro(halogeno)-substituted phenolate yttrium complex **1b** has to be used to enable access to isotactic PBPL^{FG}s (Scheme 4). Would these two conditions not be simultaneously satisfied, either atactic (most typically using **1a**) or syndio-enriched (commonly prepared from **1c** or **1d**) PBPL^{FG}s would be recovered. The screening of this whole range of FGs in the evaluation of the efficiency of the stereoselectivity of the typical catalyst systems based on **1a–d** hence confirms that the combined stereoelectronic contribution of the lactone-substituent FG and of the catalyst substituents R, along with possible NCIs between FG and R, are all determinant and interdependent. This fine *FG*···*R* cooperation is ultimately confirmed as being the key parameter to understand and tune the fine microstructure of functional and non-functional PHAs prepared by chemical ROP of the β-lactone monomers.

Conflicts of interest

The authors declare no conflict of interest.

Acknowledgements

We are grateful for the financial support provided by the University of Rennes and Lebanese University (Ph.D. grants to R. M. S. and A. D.). We thank Jérôme Ollivier and Philippe Jéhan, and Christine Deponge and Elsa Caytan for MS and NMR analyses, respectively, partly developed at ScanMAT UAR 2025 CNRS-Université de Rennes.

References

1 L. Al-Shok, D. M. Haddleton and F. Adams, *Advances in Polymer Science*, Springer, Berlin, Heidelberg, 2022. DOI: 10.1007/12_2021_111.
2 E. Glöckler, S. Ghosh and S. Schulz, *Polym. Rev.*, 2023, **63**, 478–514.
3 Yu. Wang, X. Wang, W. Zhang and W. H. Sun, *Organometallics*, 2023, **42**, 1680–1692.
4 D. J. Walsh, M. G. Hyatt, S. A. Miller and D. Guironnet, *ACS Catal.*, 2019, **9**, 11153–11188.
5 M. J.-L. Tschan, R. M. Gauvin and C. M. Thomas, *Chem. Soc. Rev.*, 2021, **50**, 13587–13608.
6 W. Josh, P. Hannah, J. Setuhn, B. Panagiotis, B. Matthew and D. Andrew, *Nat. Rev. Chem.*, 2019, **3**, 514–535.
7 H. Li, R. M. Shakaroun, S. M. Guillaume and J.-F. Carpentier, *Chem. – Eur. J.*, 2020, **26**, 128–138.
8 S. M. Guillaume, E. Kirilov, Y. Sarazin and J.-F. Carpentier, *Chem. – Eur. J.*, 2015, **21**, 7988–8003.
9 J.-F. Carpentier, *Organometallics*, 2015, **34**, 4175–4189.
10 A. Amgoune, C. M. Thomas, S. Ilinca, T. Roisnel and J.-F. Carpentier, *Angew. Chem., Int. Ed.*, 2006, **45**, 2782–2784.
11 R. Ligny, M. M. Hänninen, S. M. Guillaume and J.-F. Carpentier, *Chem. Commun.*, 2018, **54**, 8024–8031.
12 R. M. Shakaroun, A. Dhaini, R. Ligny, A. Alaaeddine, S. M. Guillaume and J.-F. Carpentier, *Polym. Chem.*, 2023, **14**, 720–727.
13 R. M. Shakaroun, H. Li, P. Jéhan, M. Blot, A. Alaaeddine, J.-F. Carpentier and S. M. Guillaume, *Polym. Chem.*, 2021, **12**, 4022–4034.
14 R. Ligny, S. M. Guillaume and J.-F. Carpentier, *Chem. – Eur. J.*, 2019, **25**, 6412–6424.
15 R. Ligny, M. M. Hänninen, S. M. Guillaume and J.-F. Carpentier, *Angew. Chem., Int. Ed.*, 2017, **56**, 10388–10393.
16 C. G. Jaffredo, Y. Chapurina, E. Kirillov, J.-F. Carpentier and S. M. Guillaume, *Chem. – Eur. J.*, 2016, **22**, 7629–7641.
17 C. G. Jaffredo, Y. Chapurina, S. M. Guillaume and J.-F. Carpentier, *Angew. Chem., Int. Ed.*, 2014, **53**, 2687–2691.
18 Note that the isoselective ROP of BPL^{Me} (*i.e.*, β-butyrolactone) was previously reported from other catalytic systems. Refer to: (*a*) J. Bruckmoser, S. Pongratz, L. Stieglitz and B. Rieger, *J. Am. Chem. Soc.*, 2023, **145**,

11494–11498; (*b*) X. Dong, A. M. Brown, A. J. Woodside and J. R. N. Robinson, *Chem. Commun.*, 2022, **58**, 2854–2857; (*c*) X. Dong and J. R. Robinson, *Chem. Sci.*, 2020, **11**, 8184–8195; (*d*) Z. Zhuo, C. Zhang, Y. Luo, Y. Wang, Y. Yao, D. Yuan and D. Cui, *Chem. Commun.*, 2018, **54**, 11998–12001; (*e*) S. Vagin, M. Winnacker, A. Kronast, P. T. Altenbuchner, P. Deglmann, C. Sinkel, R. Loos and B. Rieger, *ChemCatChem*, 2015, **7**, 3963–3971; (*f*) N. Ajellal, G. Durieux, L. Delevoye, G. Tricot, C. Dujardin, C. M. Thomas and R. M. Gauvin, *Chem. Commun.*, 2010, **46**, 1032–1034; (*g*) R. Reichardt, S. Vagin, R. Reithmeier, A. K. Ott and B. Rieger, *Macromolecules*, 2010, **43**, 9311–9317; (*h*) M. Zintl, F. Molnar, T. Urban, V. Bernhart, P. Preishuber-Pflugl and B. Rieger, *Angew. Chem., Int. Ed.*, 2008, **47**, 3458–3460.

19 L. Marshall, V. C. Gibson and H. S. Rzepa, *J. Am. Chem. Soc.*, 2005, **127**, 6048–6051.

20 S. Gesslbauer, R. Savela, Y. Chen, A. J. P. White and C. Romain, *ACS Catal.*, 2019, **9**, 7912–7920.

21 H.-Y. Huang, W. Xiong, Y.-T. Huang, K. Li, Z. Cai and J.-B. Zhu, *Nat. Catal.*, 2023, **6**, 720–728.

22 J.-F. Brière, S. Oudeyer, V. Dallab and V. Levacher, *Chem. Soc. Rev.*, 2012, **41**, 1696–1707.

23 O. I. Kazakov, P. P. Datta, M. Isajani, E. T. Kiesewetter and M. K. Kiesewetter, *Macromolecules*, 2014, **47**, 7463–7468.

24 M. E. G. Mosquera, M. P. Cebrián and M. F. Millan, Influence of Noncovalent Interactions in Catalytic Ring-opening Polymerization Processes, in *Noncovalent Interactions in Catalysis*, RSC Catal. Ser., 2019, ch. 19.

25 X. Tang, A. H. Westlie, E. M. Watson and E. Y.-X. Chen, *Science*, 2019, **366**, 754–758.

26 X. Tang and E. Y.-X. Chen, *Nat. Commun.*, 2018, **9**, 2345.

27 A. H. Westlie, S. A. Hesse, X. Tang, E. C. Quinn, C. R. Parker, C. J. Takacs, C. J. Tassone and E. Y.-X. Chen, *ACS Macro Lett.*, 2023, **12**, 619–625.

28 Z. Zhang, C. Shi, M. Scoti, X. Tang and E. Y.-X. Chen, *J. Am. Chem. Soc.*, 2022, **144**, 20016–20024.

29 X. Tang, A. H. Westlie, L. Caporaso, L. Cavallo, L. Falivene and E. Y.-X. Chen, *Angew. Chem., Int. Ed.*, 2020, **20**, 7881–7890.

30 A. H. Westlie and E. Y.-X. Chen, *Macromolecules*, 2020, **53**, 9906–9915.

31 H. Westlie, E. C. Quinn, C. R. Parker and E. Y.-X. Chen, *Prog. Polym. Sci.*, 2022, **134**, 101608.

32 *Fluorinated Polymers: Synthesis and Applications, Organofluorine Compounds*, ed. R. Schwarz and C. E. Diesendruck, John Wiley & Sons, Ltd., 2022, DOI: **10.1002/9780470682531.pat1008**.

33 B. Ameduri and H. Sawada, *Fluorinated Polymers*, The Royal Society of Chemistry, Cambridge, 2017, vol. 2, p. 372.

34 G. Hougham, P. E. Cassidy, K. Johns and T. Davidson, *Fluoropolymers 2: Properties*, Kluwer/Plenum, New York, 1999.

35 J. Scheirs, in *Modern Fluoropolymers*, ed. J. Scheirs, John Wiley & Sons, New York, 1997, ch. 24, pp. 435–486.

36 B. W. Thuronyi, T. M. Privalsky and M. C. Y. Chang, *Angew. Chem., Int. Ed.*, 2017, **56**, 13637–13640.

37 Y. Takagi, R. Yasuda, A. Maehara and T. Yamane, *Eur. Polym. J.*, 2004, **40**, 1551–1557.

38 O. Kim, R. A. Gross, W. J. Hammar and R. A. Newmark, *Macromolecules*, 1996, **29**, 4572–4581.

39 M. Le Gal, A. Rios De Anda, L. Michely, C. S. Colin, E. Renard and V. Langlois, *Biomacromolecules*, 2021, **22**, 4510–4520.

40 G. Foli, M. D. Esposti, M. Toselli, D. Morselli and P. Fabbri, *Analyst*, 2019, **144**, 2087–2096.

41 J. W. Kramer and G. W. Coates, *Tetrahedron*, 2008, **64**, 6973–6978.

42 T. Xu, G. Yang, C. Liu and X. Lu, *Macromolecules*, 2017, **50**, 515–522.

43 J. W. Kramer, E. B. Lobkovsky and G. W. Coates, *Org. Lett.*, 2006, **8**, 3709–3712.

44 J. Wöltinger, J. E. Bäckvall and Á. Zsigmond, *Chem. – Eur. J.*, 1999, **5**, 1460–1467.

45 W. F. Edgell and J. Lyford IV, *Inorg. Chem.*, 1970, **9**, 1932–1933.

46 M. Bochmann, G. Bwembya and K. J. Webb, *Inorg. Synth.*, 1997, **31**, 19–24.

47 B. M. Chamberlain, M. Cheng, D. R. Moore, T. M. Ovitt, E. B. Lobkovsky and G. W. Coates, *J. Am. Chem. Soc.*, 2001, **123**, 3229–3238.

48 S. E. Schaus, B. D. Brandes, J. F. Larrow, M. Tokunaga, K. B. Hansen, A. E. Gould, M. E. Furrow and E. N. Jacobsen, *J. Am. Chem. Soc.*, 2002, **124**, 1307–1315.

49 J. A. Schmidt, E. B. Lobkovsky and G. W. Coates, *J. Am. Chem. Soc.*, 2005, **127**, 11426–11435.

50 The value of P_r = 0.09 for the isotactic-enriched polymer evidences stereoerrors that arise from the incomplete enantiopurity of the initial monomer (*S*)-BPL^{CH_2OCF_2CHF_2} which was prepared from the corresponding enantio-enriched epoxide G^{CH_2OCF_2CHF_2}, obtained itself by hydrolytic kinetic resolution of the racemic compound (refer to the ESI, Scheme 1†); the latter epoxide was clearly much enantio-enriched but, despite our efforts, chiral GLC did not enable us to achieve complete separation of the peaks of two enantiomers and thus to provide an accurate value of % ee; the enantiopurity of epoxide G^{CH_2OCF_2CHF_2}, and therefore of monomer (*S*)-BPL^{CH_2OCF_2CHF_2}, is estimated to >90% ee.

51 H. Li, J. Ollivier, S. M. Guillaume and J.-F. Carpentier, *Angew. Chem., Int. Ed.*, 2022, **61**, e202202386.

52 R. M. Shakaroun, H. Li, P. Jéhan, A. Alaaeddine, J.-F. Carpentier and S. M. Guillaume, *Polym. Chem.*, 2020, **11**, 2640–2652.

53 N. Ajellal, M. Bouyahyi, A. Amgoune, C. M. Thomas, A. Bondon, I. Pillin, Y. Grohens and J.-F. Carpentier, *Macromolecules*, 2009, **42**, 987–993.

